A Prototype Gas Analysis System Using a Miniature Gas Chromatograph

Interagency
Energy/Environment
R&D Program
Report

A PROTOTYPE GAS ANALYSIS SYSTEM USING

A MINIATURE GAS CHROMATOGRAPH

Professor James B. Angell, Principal Investigator
John H. Jerman
Stephen C. Terry, Ph.D.
Soheil Saadat
Integrated Circuits Laboratory
Stanford Electronics Laboratory
Stanford University
Stanford, California 94305

DISCLAIMER

Mention of company name or product does not
constitute endorsement by the National Institute
for Occupational Safety and Health.

Dr. Laurence J. Doemeny
NIOSH Project Officer

ABSTRACT

The techniques of integrated circuit processing have been utilized to miniaturize the main components of a gas chromatography system. A 1.5-m long separating column, sample injection valve, and output thermal conductivity detector are all fabricated on a single 5-cm diameter silicon wafer. These components are combined with a sophisticated microcomputer system, consisting of a microprocessor, solid state memory, analog-to-digital converter, keyboard, and display, to form an advanced, portable gas analysis and data logging system. The system can automatically sample the air, measure the concentration of up to 10 contaminant vapors, calculate and store contaminant concentrations, and estimate average worker exposures. The computer system allows exceptional flexibility in the retrieval of concentration information, ease in operation, and simplicity of calibration. The instrument can be used as an exposure monitor to sample the air at 1.5 minute intervals for an 8-hour shift, or it can be used as a survey instrument to take and analyze samples and provide concentration information within 30 seconds of sampling. The small size, advanced capabilities, and ease of operation of the system should have a significant impact on the fields of industrial hygiene and occupational safety and health. The instrument will greatly expand the ability to monitor workers' exposures to toxic gases and therefore aid in the reduction of such exposures, and provide better epidemological data in future health studies.

CONTENTS

FIGURES

TABLES

1. INTRODUCTION

1.1 BACKGROUND

The miniature gas chromatographic air analyzer is a unique instrument combining a gas chromatograph fabricated on a silicon wafer and a sophisticated microcomputer system for analyzing the data and controlling the device. The development of the miniature system has depended principally on advances in the field of integrated circuit processing. The reduction in size of the gas chromatograph is due to the application of silicon etching technology to the miniaturization of the separating column, injection valve, and detector. The sophisticated electronics system needed to control the system has been made possible through the use of recently introduced one-chip microprocessors and high density, low power memory chips. The combination of these technologies results in an instrument with unique analytical and field capabilities.

There is a widespread need in the industrial hygiene field for the rapid and accurate monitoring of potentially hazardous concentrations of many gases in the air. Currently there are several types of portable, direct-reading instruments for the monitoring of single contaminants. These instruments lack the versatility needed to adequately monitor the work place. A variety of small, passive monitors are becoming available, but these either require expensive and time-consuming analysis in the laboratory or are designed for only a single contaminant. A gas chromatograph (GC), which is capable of separating, identifying, and measuring the constituents of a gaseous sample, is an ideal instrument for performing the analysis of an industrial environment. A conventional GC, however, is much to bulky to be used either for a portable survey instrument or as an exposure monitor for a mobile worker.

The reduction in size of the components of a GC realized by using silicon etching technology have made a portable instrument possible. The feasibility of such a portable instrument was studied at Stanford University under NIOSH contract #210-76-0140 [1] and a prototype, which is the subject of this report, has been fabricated. The prototype is capable of automatic, real-time analysis of atmospheric gas samples for up to 10 different vapors at concentrations down to a few parts-per-million. These instruments promise to significantly aid in the investigation of potentially harmful environments.

The work on the miniature GC started at Stanford University in 1971 in an attempt to develop a miniature instrument for NASA to fly on the Viking landers to Mars. A separating column was rapidly developed, but there was insufficient time to develop the integrated valve and detector structures

1

before the launch. The first integrated GC, which consists of a long separating column, a sample injection valve, and a thermal conductivity detector, all fabricated on a single silicon wafer, was developed in 1974 [2]. It operates by continually passing a carrier gas through the separating column. This column is lined with a material capable of adsorbing and desorbing the constituents of a gaseous sample. A brief pulse of sample gas is injected at the head of the separating column. As the constituents are swept along the column they are each retained in the lining for characteristically different total times. They thus exit from the tube as separate peaks, which are detected by the changes in thermal conductivity of the output gas stream.

The components of the integrated GC have been developed and refined in the last few years and the performance of the device has steadily improved. There have been concurrent rapid advances in the semiconductor industry in the field of miniaturized digital computers. A significant effort has been expended to apply those miniature computers to the GC system to form a portable analytical system with advanced capabilities. The computer controls the sequence of operation of the GC and implements sophisticated digital filtering, peak detection, peak area calculations, data storage, and display functions which would have been impossible in a portable package the size of the prototype before 1979.

Work has also been done to miniaturize the other parts of a total instrument, such as the carrier gas supply and sample injection system. Since the miniature GC is so much different from conventional instruments, most available components are not suitable for use in this system. The GC, support components, and electronics system have been combined to form a portable instrument, shown in Figure 1.1, about 20 cm x 22 cm x 10 cm (8" x 9" x 4"), which weighs 2.8 kg (6.2 lbs). It is capable of sampling the air automatically at specified time intervals, or on command from the operator. The instrument is programmed to look for up to 10 different constituents of the gas sample, calculate their respective concentrations, calculate and store time-weighted-average concentrations, display the concentration of any desired compound on demand, and sound an alarm if any concentration exceeds a preset level. It contains sufficient carrier gas in convenient, replaceable cartridges to last for at least four days of continuous operation and has a rechargeable battery system for up to 8 hours of operation between charges. Since the computer handles all aspects of the instrument operation, the unit is very simple to use.

Figure 1.1. PHOTOGRAPH OF THE PROTOTYPE GAS ANALYSIS SYSTEM. The package
measures about 20 cm x 22 cm x 10 cm and weighs 2.8 kg.

2. THE MINIATURE GAS CHROMATOGRAPH

The miniature gas chromatograph is the heart of the portable gas analysis
system. It separates the gaseous sample into its component vapors and
detects and measures the concentration of the separated constituents.
The miniature gas chromatograph is similar in function to larger labora-
tory chromatographs, but the method of fabrication of the components is
quite different.

2.1 INTRODUCTION TO GAS CHROMATOGRAPHY

Gas chromatography is a technique widely used in analytical chemistry for
the separation and analysis of gaseous samples. A typical gas chromato-
graph (GC) consists of a carrier gas supply, a sample injection system,
a separating column, and an output detector, as shown in the block diagram
(Figure 2.1). Separation of the sample vapors is achieved via their dif-
ferential migration through a capillary column. The sample vapors are
injected at the input of the column by a valve and are swept through it
by an inert carrier gas. The column is lined with a liquid stationary
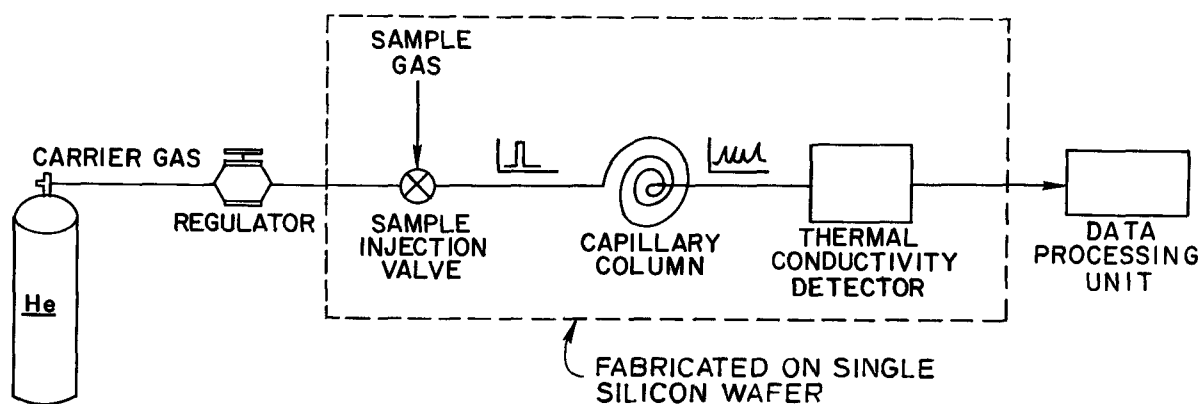
Figure 2.1. SCHEMATIC OF A SIMPLE GAS CHROMATOGRAPHY SYSTEM.

phase, a substance capable of absorbing and desorbing each of the com-
ponent vapors. The migration rate of each vapor along the column depends
on the carrier gas velocity and the degree to which the vapor is absorbed
by the stationary phase. The mixture of sample vapors, injected into the
capillary as a single pulse, is separated as it travels through the column,
with each component vapor traveling at a different rate and emerging at a

5

specific time. The column's output is thus a series of vapor peaks separated by regions of pure carrier gas. To detect these peaks, the output gas stream from the column is passed over a detector which measures a particular property of the gas, such as thermal conductivity, which can be related to the concentration of sample vapor in the carrier gas. The detector produces a signal which is amplified and recorded as a function of time. Chromatograms obtained in this manner are used in the quantitative analysis of the sample mixture since the identity and quantity of each vapor in the mixture can be determined from its retention time in the column and the area under its output peak.

2.2 SILICON ETCHING TECHNOLOGY

Miniaturization of the components of the GC requires the ability to fabricate small three-dimensional structures with tightly controlled geometries. Photolithographic techniques have been developed by the integrated circuit industry for patterning silicon with complex two-dimensional circuits with features less than 5-μm wide. The combination of these photolithographic techniques with different silicon etches has resulted in the ability to form the valves, columns, and detectors required for a miniature GC.

In larger gas chromatographs, the common practice is to fabricate the individual elements of the system as separate units, and then assemble the components into a system using connecting tubing. In the integrated GC, however, the volumes of the individual components (column, valve, and detector) are so small that any discrete tubes and connectors would contribute unacceptably large dead volumes which would excessively dilute the sample peaks. The miniature GC system must be connected with tubes of diameter nearly equal to the column diameter, which necessitates the integration of many of the system components on the same substrate. With silicon etching technology, the connecting tubes can be fabricated at the same time and with similar dimensions as the system elements, so no extra processing steps are required.

2.2.1 Etched Geometries

A wide variety of different features can be etched in silicon depending upon the shape of the mask and the type of etchant used. Fabrication of these features involves a series of oxidation, photolithography, and etching steps similar to those of standard integrated circuit processing. The basic photolithography process is depicted in Figure 2.2. A layer of silicon dioxide (SiO_2) is first grown on the wafer in a high temperature furnace. This oxide layer will serve as the etch mask in the subsequent silicon etching step. The desired pattern must then be transferred to the oxide. A thin layer of photosensitive material is spun onto the wafer. A glass photographic plate with an emulsion image of the desired pattern is placed in contact with the wafer, and the photoresist is exposed with UV light. The photoresist on the wafer is then developed, leaving the oxide protected by the resist in the desired etch mask pattern. The excess SiO_2 is etched away, leaving bare silicon where the etched feature is to be located.

Several cross-sectional profiles of grooves are available, depending upon the orientation of the groove with respect to the crystallographic planes

Silicon Dioxide

Silicon

(a)

Photoresist

(b)

↓ ↓ ↓ ↓ UV

Mask (glass)

(c)

Glass

(d)

(e)

(f)

(g)

Figure 2.2.   THE STEPS IN THE PHOTOLITHOGRAPHIC PROCESS ARE: (a) a thin
layer of SiO$_2$ is thermally grown on the silicon surface;
(b) a layer of photosensitive material is spun onto the oxide
layer; (c) a glass mask is placed in contact with the wafer
and exposed to UV light; (d) the glass mask has a negative
image of the desired pattern; (e) the unexposed photoresist
is developed away; (f) the oxide layer is etched in buffered
HF; and (g) the photoresist is chemically removed.

of the silicon, the type of etchant used, and the conditions under which
the etch is performed. An anisotropic etchant such as potassium hydroxide
(KOH) in water will produce V-shaped grooves in (100) oriented silicon,
as shown in Figure 2.3a. This etchant will not attack the (111) crystal
planes in silicon, which form the V-walls. For a relatively narrow groove,
where the V-walls meet at the bottom, the depth of the grooves can be

7
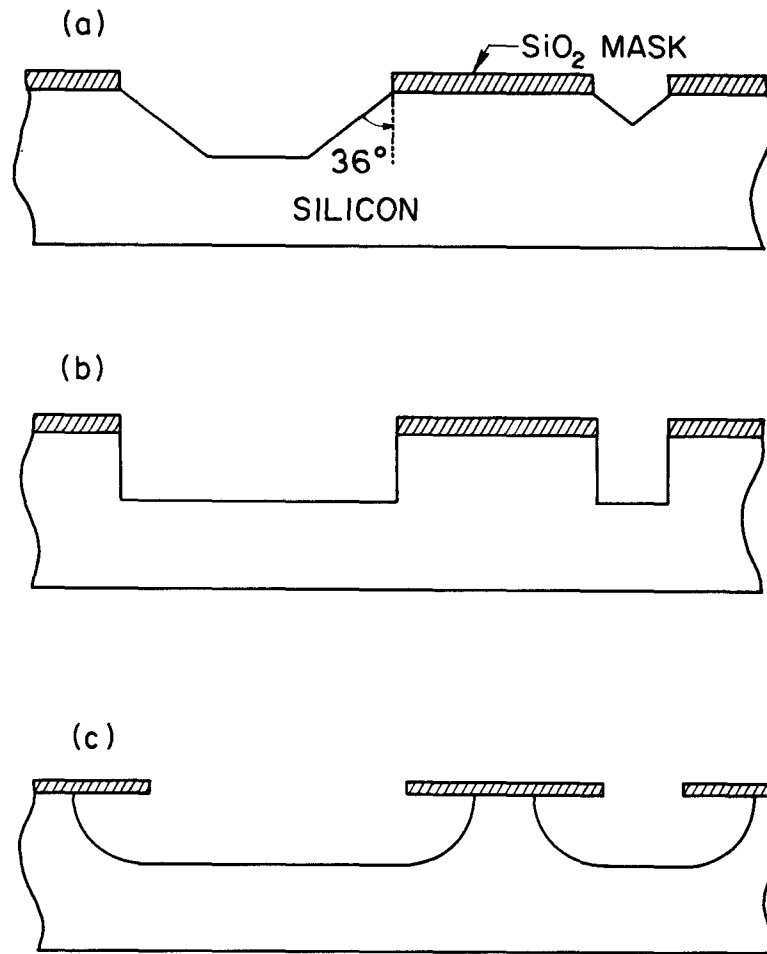
Figure 2.3. REPRESENTATIVE ETCHED CROSS SECTIONS IN Si.
(a) Grooves etched with KOH and water in (100)
Si. (b) Grooves etched with KOH and water in
(110) Si. (c) Grooves etched with HF-nitric
solutions in Si.

precisely determined by the initial width of the etch mask. In (110)
oriented silicon and along certain directions in (100) silicon, a KOH
etch will produce grooves with precisely vertical walls as shown in
Figure 2.3b. The choice of geometries is limited with these etches
because of their dependence upon the crystal structure of the silicon,
so that some desired features, such as round holes with vertical walls,
cannot be realized.

A mixture of hydrofluoric and nitric acids can be used as an isotropic
etchant to produce grooves as shown in Figure 2.3c. This etchant is
used in forming many of the features of the miniature GC system since it
produces nearly rectangular grooves, oriented in any direction of the
wafer.

8

A sequence of these isotropic and anisotropic etches is used to form the substrate GC wafer. Though described separately below, many of these etches for the valve, capillary column, and detector gas channel can be performed simultaneously, reducing the total number of necessary photolithographies and etches. The detector chip is removable from the substrate wafer and is batch fabricated on separate wafers using similar etching techniques.

2.3 MINIATURE GC FABRICATION

2.3.1 Capillary Column

The miniature capillary column is formed by etching a long, narrow spiral groove into the surface of a silicon wafer and then hermetically sealing the wafer to a Pyrex glass cover plate. The capillary column is the prominent feature in Figure 2.4, a photograph of the GC wafer. Most of the miniature GC's produced have used capillary columns 1.5-m long, about 200-μm wide, and 30-μm to 55-μm deep. Holes etched through the wafer at the ends of the column serve as entrance and exit ports for the carrier gas.
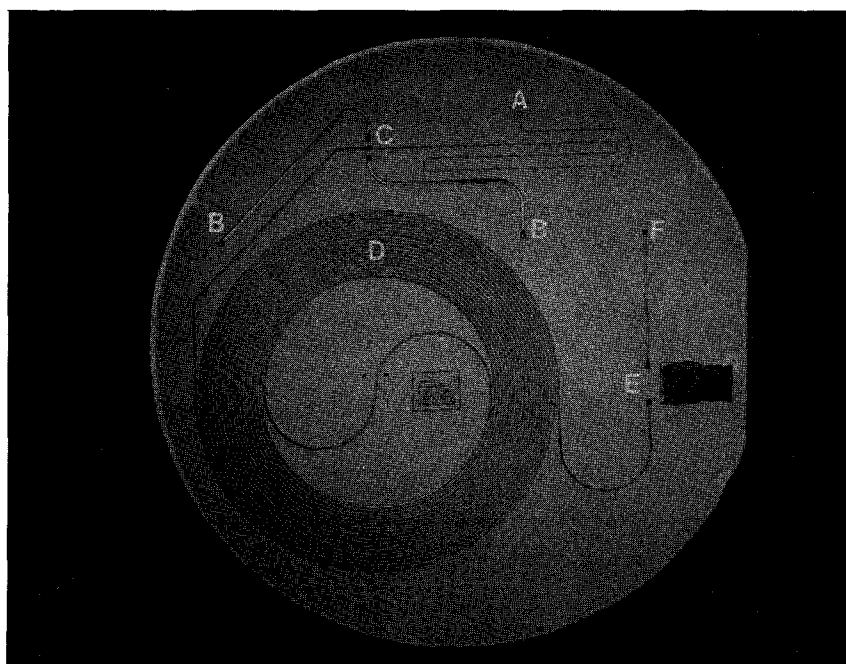
Figure 2.4. PHOTOGRAPH OF THE GC WAFER. The view is through the 5-cm square Pyrex cover glass. (A) Carrier gas input feedthrough hole. (B) Sample gas input and exit feedthrough holes. (C) Sample injection valve, backside of wafer. (D) 1.5-m long separating column. (E) Detector gas channel, backside. (F) Vent to atmosphere.

9

The capillary column and gas feedthrough ports are fabricated in two separate photolithographic and etching steps. The starting material is a 200-μm thick, 5-cm diameter silicon wafer of (100) surface orientation. The capillary column is first formed by transferring the 1.5-m long folded spiral into a 1-μm thick layer of SiO_2. Since the spiral does not follow any particular crystallographic direction, an isotropic HF-nitric acid etchant is then used to etch the spiral groove into the silicon. The remaining SiO_2 is then removed, and more SiO_2 is grown as the etch mask for the feedthrough hole etch. The holes are etched through the wafer using an anisotropic etchant in order to minimize their volume.

The wafer is again stripped of the remaining oxide and is placed in contact with a 5-cm square piece of Pyrex glass. A relatively low temperature anodic bonding process is used to hermetically seal the wafer to the glass. The silicon and glass are heated to about 400°C and a potential of 600 V is applied to the structure. The resulting electrostatic field pulls the two materials together, and a bond is quickly formed. The seal between the glass and silicon is hermetic and irreversible, thus forming the etched spiral groove into an enclosed capillary tube. This unlined capillary column must be coated with a column lining before any chromatographic separations can be obtained. The methods of column lining will be discussed in Section 4.5.1.

2.3.2 Sample Injection Valve

The purpose of the sample injection valve is to introduce a very brief pulse of sample gas into the carrier gas stream at the head of the capillary column. For the miniature GC, the volume of injected sample is about 10 nl, which generally requires that the valve remain open for about 5 ms. This volume of injected sample is about three orders of magnitude smaller than what can be obtained with the smallest commercial valves and connecting tubing, so a custom, integrated one-valve injection system has been developed for use with the GC column.

This injection system uses a miniature, normally closed, solenoid-actuated diaphragm valve with an etched silicon valve seat, as shown in Figure 2.5. The valve seat is fabricated using two isotropic silicon etches on the opposite side of the wafer from the capillary column. The details of the etched valve seat can be seen in the SEM photograph, Figure 2.6. The nickel diaphragm is held against the valve sealing ring by the body of the solenoid. An adjustable compression spring normally forces the solenoid plunger and diaphragm against the valve seat. When the solenoid is energized, the plunger is pulled back into the body of the solenoid, allowing the diaphragm to relax. The gas on the input side of the valve is held at a slightly higher pressure than the output, so that the gas is forced over the valve seat, injecting a pulse of gas into the capillary column. When the solenoid is turned off, the plunger again forces the diaphragm against the valve seat, stopping the flow of gas. Since the valve is fabricated directly on top of the capillary column, there is little dead volume associated with the feedthrough hole connecting the valve seat and the column. The volume of the feedthrough hole on the output of the valve is only about 4 nl, and this volume is swept quickly by the 2 to 5 μl/s carrier gas flow. Experiments with this valve design
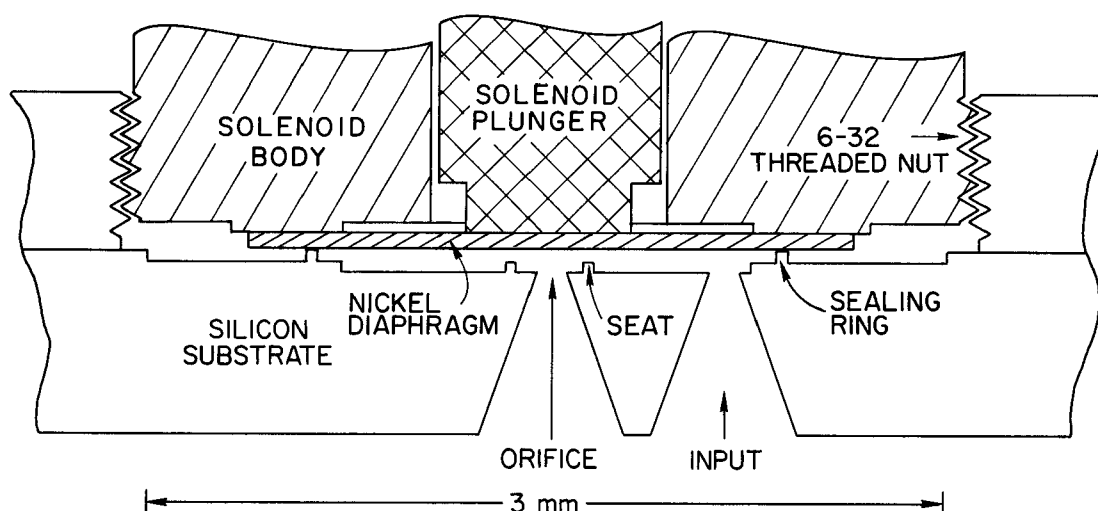
Figure 2.5. CROSS-SECTIONAL VIEW OF SAMPLE INJECTION VALVE. Vertical scale exaggerated for clarity.

on very short columns have not shown any tailing of the injected pulse due to valve dead volumes. Several valves have been put through a million operations with no detectable change in performance.

Figure 2.6. SEM PHOTOGRAPH OF AN ETCHED SILICON VALVE SEAT. (A) Feedthrough hole to capillary column. (B) Valve seating ring. (C) Feedthrough holes to sample input channels. (D) Valve sealing ring.

11

2.3.3 Detector Configuration and Fabrication

After an extensive review of GC detector technology, a thermal conductivity detector (TCD) was chosen for use in the integrated gas chromatograph. The advantages of the TCD include fast and general response, ease in fabrication and adaptation to the miniature system, ruggedness, and simplicity of support electronics. The detector was designed to be removable from the substrate GC wafer so that it could be cleaned or replaced in the event of detector contamination or failure.

The detector structure is shown in cross section in Figure 2.7. The gas flowing through the capillary column exists through a feedthrough hole to the detector gas channel. The separate detector chips are mechanically clamped to the backside of the GC wafer, forming one side of the detector channel. The sensing element is a thin-film nickel resistor which is supported by a thin Pyrex glass membrane. This glass membrane supports the resistor and forms one wall of the gas channel. The resistor is heated by an external current source, and its temperature is monitored by measuring the voltage dropped across the resistor. When a sample peak passes by the detector, the thermal conductivity of the carrier gas is decreased, which causes a corresponding increase in the temperature of the detector. This temperature increase causes the detector voltage to increase which is a measure of the concentration of the sample gas. The operation of the detector is covered in more detail in Section 4.3.
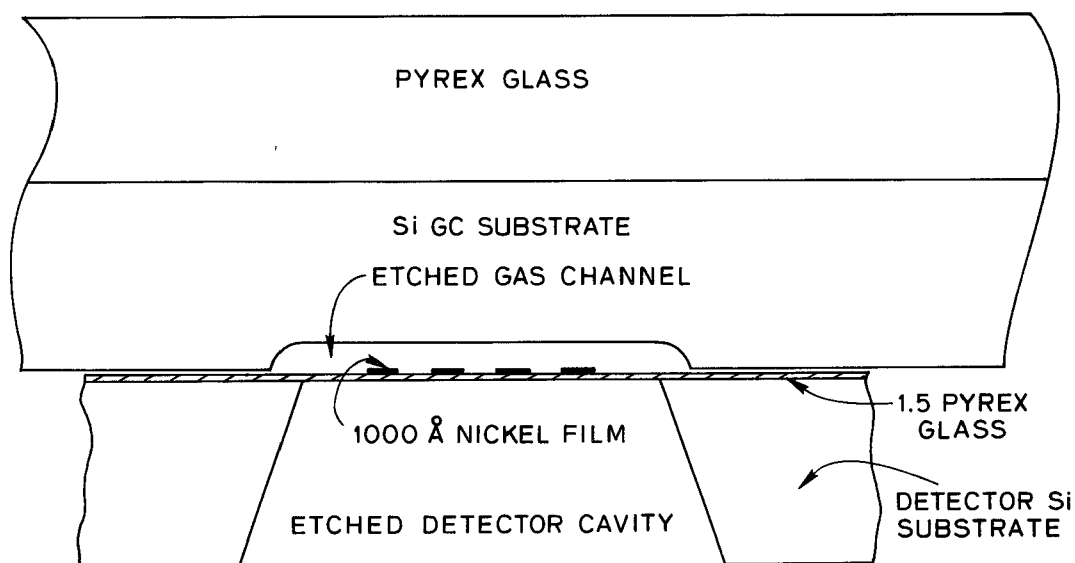
Figure 2.7. CROSS-SECTIONAL VIEW OF DETECTOR STRUCTURE. Vertical scale exaggerated for clarity.

The detector chips are separately batch fabricated using integrated circuit processing techniques and silicon etches. The starting wafers are 200-μm

12

thick, (100) silicon. About 1000 $\overset{o}{A}$ of SiO_2 is thermally grown on the wafer followed by the sputter deposition of about 1.5-μm of Pyrex. Large holes, about 300-μm by 700-μm are etched from the back of the wafers to remove the thermally conductive silicon from the detector region. About 1000 $\overset{o}{A}$ of nickel is evaporated on the Pyrex membrane, defined photolithographically, and etched to produce the detector resistor. The chips are then sawn apart and lead wires are bonded to the resistor to complete the fabrication process.

3. INSTRUMENT SYSTEM

The gas chromatographic air analyzer is a system built around two key components, the miniature gas chromatograph and a powerful microcomputer. The chromatograph separates and detects the components of a gaseous sample and the computer analyzes and displays the output of the chromatograph and controls the operation of the entire system.

A block diagram of the system is shown in Figure 3.1. The chromatographic section includes the integrated GC described in Chapter 2 plus the sample pump and injection system, a 15-cm^3 high pressure helium supply and a pressure regulator. The electronics section includes analog electronics to amplify the detector output, other pressure and temperature sensors, and digital electronics to process those signals, display the results, and sequence and control the GC system.
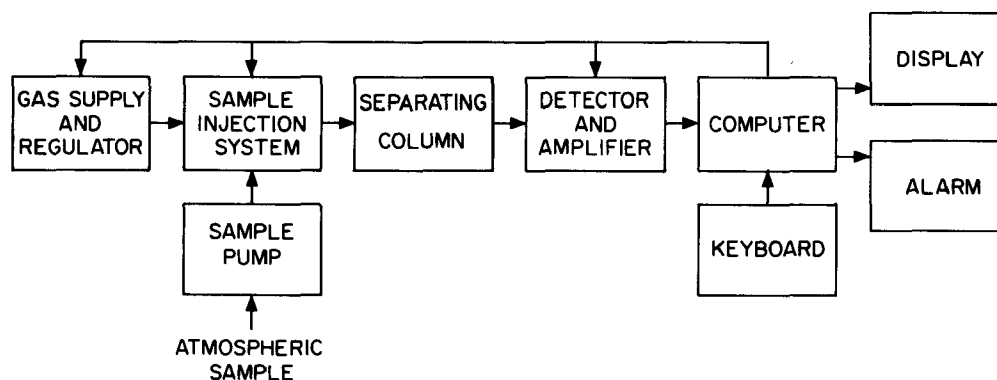
Figure 3.1. BLOCK DIAGRAM OF PROTOTYPE GAS ANALYSIS SYSTEM.

3.1 CARRIER GAS SUPPLY

The carrier gas supply is shown in the block digram of Figure 3.2. The high pressure helium is passed through a resistive gas path to a high pressure valve. The pressure in a surge tank downstream from the valve is monitored by a pressure transducer. As carrier gas flows from the surge tank through the column, the pressure in the surge tank falls very slowly. Before the injection of a sample pulse in the GC, the high pressure valve is activated until the pressure in the tank reaches a preset valve. The computer then closes the high pressure valve and begins the sample injection process. This pressure regulator system works over a

15
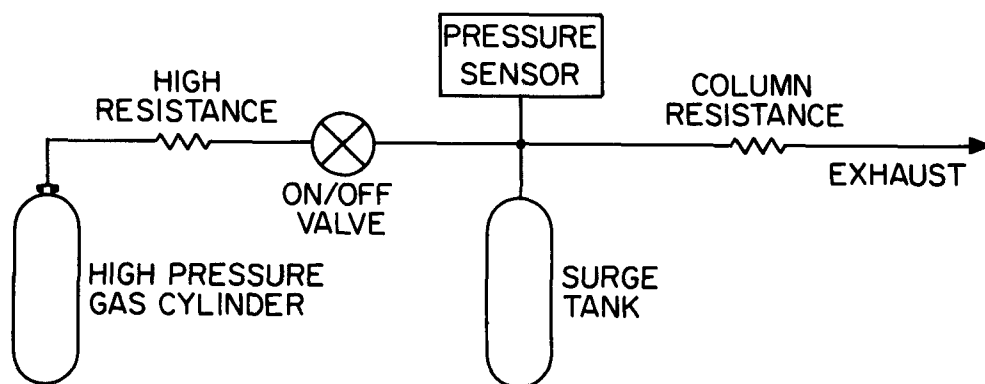
Figure 3.2. SCHEMATIC OF THE CARRIER GAS SUPPLY SYSTEM.

a wide range of helium source pressures and provides a nearly constant
carrier gas supply to the GC. With a 15-cm^3 surge tank and the nominal
3 $\mu l/s$ carrier gas flow, the carrier supply pressure will drop about
7 x 10^2 Pa (0.1 psi) during the course of an analysis.

3.2 SAMPLE INJECTION SYSTEM

The sample injection system chosen for the GC is the simple one-valve
system shown in Figure 3.3. An atmospheric sample is drawn through a
check valve and through the input side of the injection valve by a servo-
driven piston pump. After about 0.6 cm^3 of sample has been gathered, the
pump reverses, pressurizing the gas sample. When the pressure of the
sample reaches a predetermined value, the computer opens the injection
valve for a few milliseconds, causing a few nanoliters of sample to be
injected as a brief plug of gas at the head of the separating column.
The remainder of the sample is bled off from the pump before the next
sample is taken. The pump is capable of reaching pressures as high as
3.8 x 10^5 Pa (55 psig) although typical injection pressures are around
1.7 x 10^5 Pa (25 psig).

3.3 ANALOG ELECTRONICS

The primary purpose of the analog electronics section is to condition the
outputs of the various sensors in the system, including the GC detector,
for use by the microprocessor. The main portion of the analog electronics
is involved in driving and amplifying the detector. A block diagram of
the detector electronics is shown in Figure 3.4. A constant current
source is used to heat the nickel film resistor. Another current source
drives a reference resistor to reduce the effect of power supply variations
on the output. The difference between the reference voltage output and
the detector output is amplified by a gain of 5 and then fed into a high
gain, auto-zeroing amplifier. The auto-zeroing feature is important for
the high gain amplifier since the ambient temperature of the GC column
is not controlled. At a total gain of about 5000, the amplified detector
output would drift beyond the dynamic range of the amplifier due to small
changes in ambient temperature. The high gain amplifier is zeroed before
each chromatogram to keep its output within the range of the analog to

16
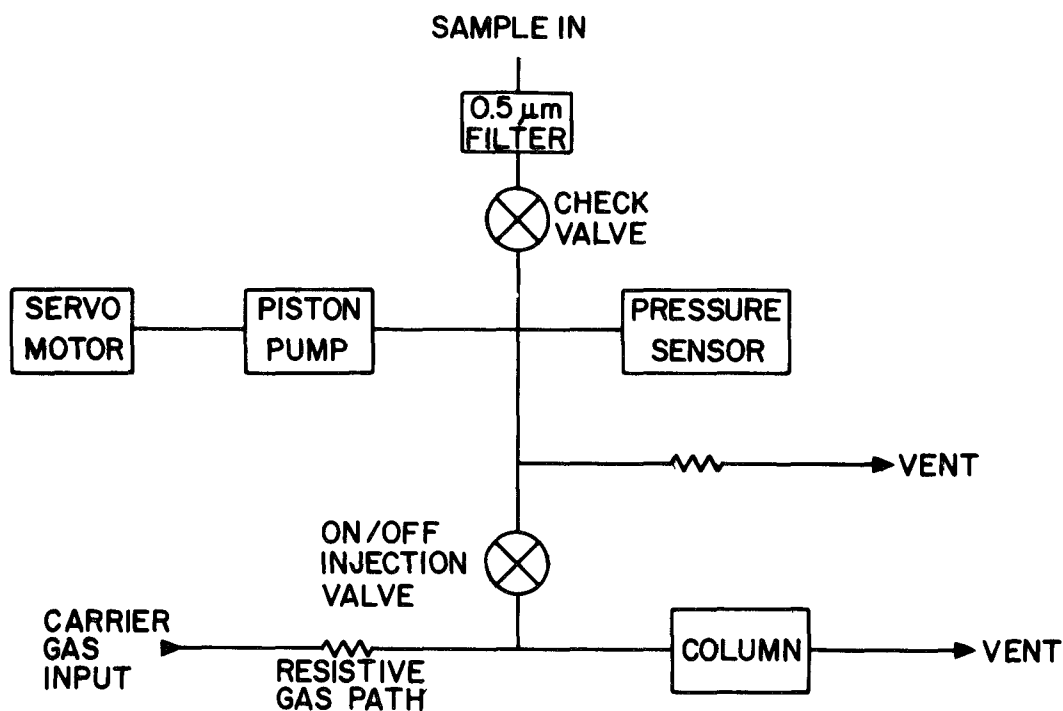
Figure 3.3.   SAMPLE INJECTION SYSTEM.

DETECTOR ELECTRONICS
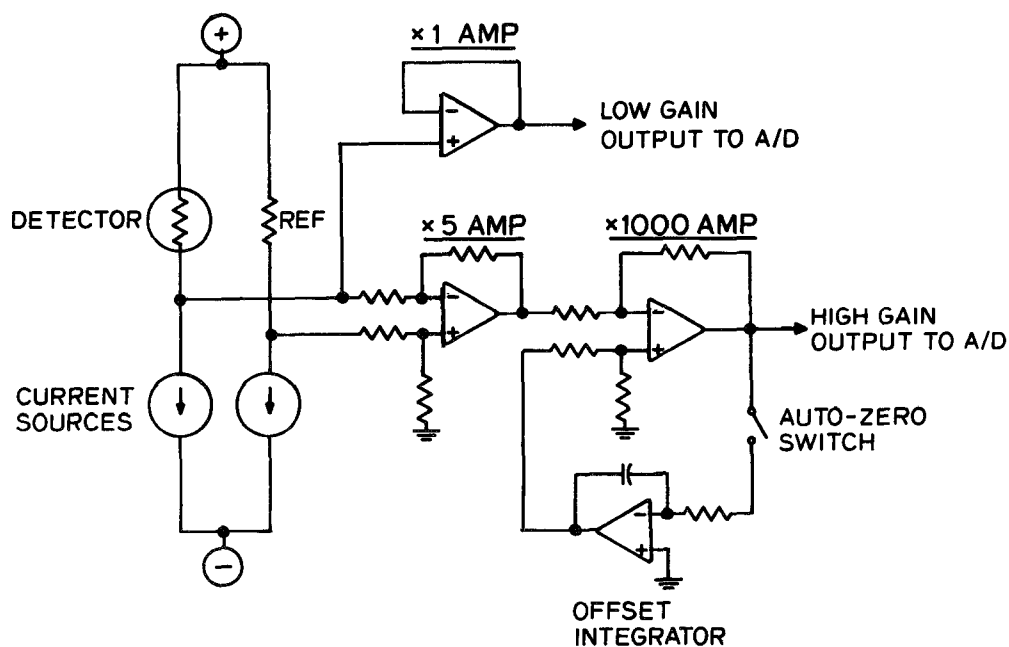
Figure 3.4.   SCHEMATIC OF DETECTOR CURRENT SOURCE AND DETECTOR AMPLIFIERS.

17

digital (A/D) converter. A low gain amplifier is also connected directly
to the detector to monitor the 1-volt air peak signals, which saturate
the high gain amplifier.

The A/D converter is the primary way that the computer obtains information
from the analog electronics. It is switched among the various pressure
sensor amplifier outputs and other signals as shown in Figure 3.5. The
pressure sensor outputs are used to control the operation of the carrier
gas supply and the sample injection system. A thermistor is used to
measure the column temperature in order to calculate the expected reten-
tion time of the sample peaks.
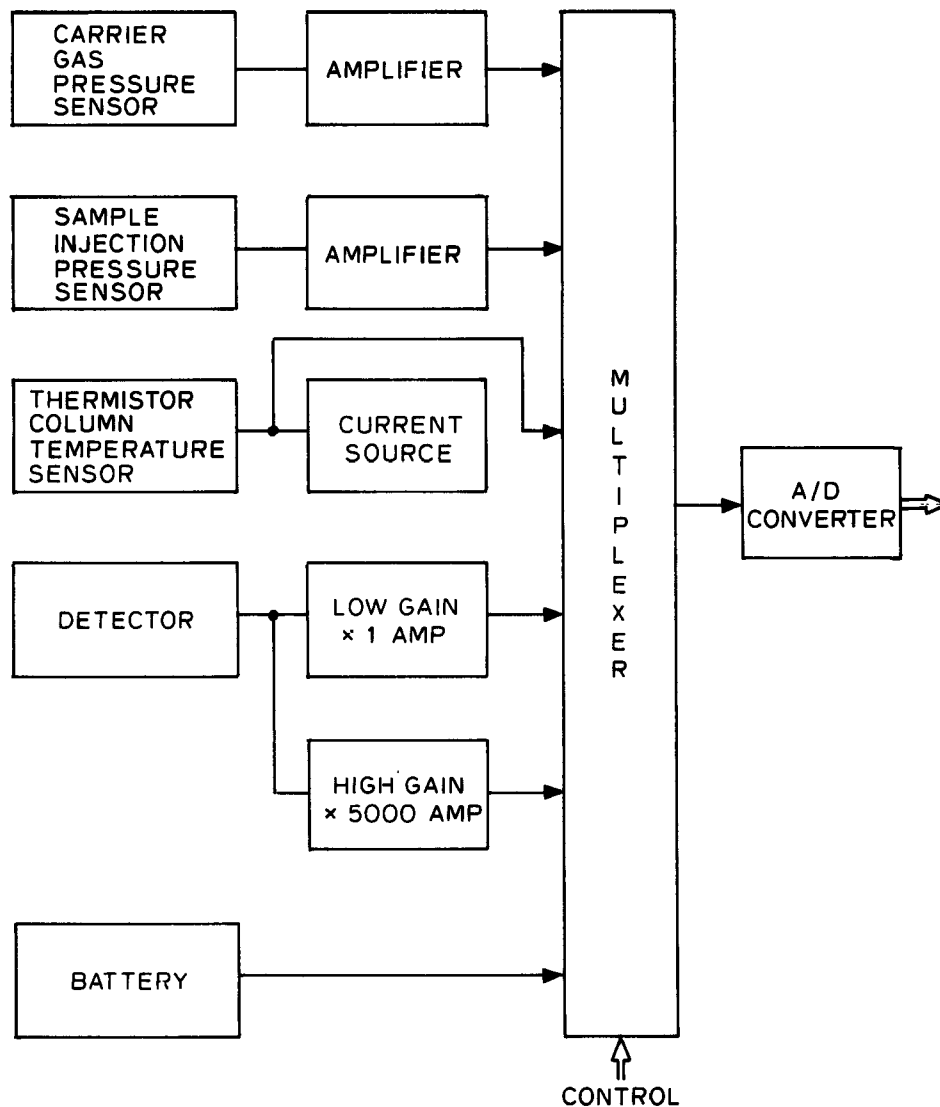
Figure 3.5. A/D CONVERTER AND MULTIPLEXER SYSTEM.

The remainder of the analog electronics allows the computer to drive the sample pump, injection valve and pressure regulator valve. In addition there are voltage references and regulators to stabilize the battery voltages and provide drive signals for the pressure and temperature sensors.

3.4 DIGITAL ELECTRONICS

The digital electronics package consists of a microprocessor chip, its associated program and data memories, a keyboard interface, and a liquid crystal display, as shown in Figure 3.6.

COMPUTER SYSTEM
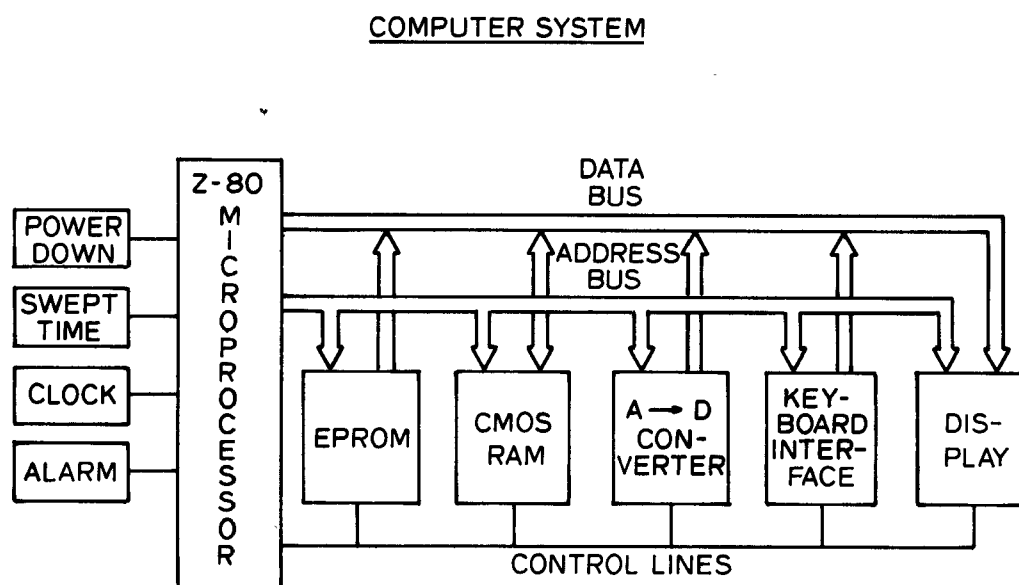
Figure 3.6. DIGITAL ELECTRONICS BLOCK DIAGRAM.

The microprocessor chosen for the system is a Zilog Z-80a. It is a relatively high speed, 8-bit device with an advanced instruction set. Since the power dissipation of this device is relatively high (1 Watt), a unique powerdown system is used to minimize the time during which power is applied to the high power consuming portions of the system. It is anticipated that functionally equivalent Z-80 devices will be available in 1981 which will dissipate about 20% of the present power. This advance will be a significant help in extending the battery life of the system or reducing the present battery size.

The computer's memory is divided into two sections, permanent program memory and volatile random access memory. The program for the computer is held in 10 kilo-bytes of electrically programmable read-only memory, EPROM. Since there is no reason to change the program during its use, the EPROM is programmed once and will store the program almost indefinitely. The volatile memory is used by the computer as a scratch pad for calculations and to store system parameters, gas parameters, and data on the

19

concentrations which it has determined. These results are held in 2 kilo-bytes of extremely low power CMOS memory which is powered continuously, even when the machine is "turned off". The keyboard allows the user to completely control the operation of the instrument by displaying and by modifying the parameters which are used by the computer to control the instrument.

In addition to the interfaces with the analog electronics, the digital system includes a 16 function keyboard and a 4-digit liquid crystal display. The keyboard offers multiple levels of control depending upon key sequence. It can be used to retrieve the sample gas concentrations, input calibration data to the computer, control the operation of the machine, and retrieve other important parameters such as carrier gas pressure, temperature, and peak retention times. The display is used to output all computer data and to check the accuracy of inputted calibration parameters.

3.5 PACKAGE

The complete instrument is housed in a package about 20 cm x 22 cm x 10 cm (8" x 9" x 4") which weighs 2.8 kg (6.2 lbs). The details of the physical layout of the package are shown in Figure 3.7 and in the photograph, Figure 3.8. A majority of the volume and weight of the present package is taken up by batteries and electronics boards. It is anticipated that the present battery weight of 765 gm, which is 27% of the total, will be reduced by a factor of about 2 when the lower power digital components become available. The volume associated with the electronics can be reduced by at least a factor of 2 by using multilayer printed circuit boards. Since the digital system design is still subject to modification as improved components become available, wire-wrap techniques, which are more easily changed than printed circuit boards, are presently used in the prototype instruments. It is further anticipated that new interface and memory components will become available which could be used to further reduce the size of the electronics boards.

The computer controls the entire system, so there is no need for user adjustable flow controls, zero controls, or meters to read. The front panel only contains a keyboard to interface with the computer, a mode switch to select automatic or survey mode, and the digital display. The only maintenance tasks are replacing the high pressure helium cartridges and recharging the batteries. The high pressure helium cartridges are changed by removing the empty cartridge from a holder on the bottom of the unit and placing a full cartridge in the holder. A screw is then rotated, forcing the cartridge against a puncturing needle and a sealing gasket. The entire operation takes less than 1 minute, and the helium cartridges are available from a commercial source for about $1.75 in quantities of 1000. Since the cartridge lasts for at least 4 days of operation, the helium operating costs are quite modest.

The complete GC subsystem occupies about 15% of the present instrument package and a similar percentage of the weight. The GC system could be separated from the electronics, if a worker-wearable version of the system is desired. The GC could then be worn by the worker near the breathing zone,

20

ANALOG CIRCUITRY

MINIATURE
G C

TOP VIEW: MIDDLE LAYER

DIGITAL ELECTRONICS
AND COMPUTER BOARD

MINIATURE
G C
HOUSING

TOP VIEW: TOP LAYER

20 cm

6 V BATTERY

6 V BATTERY

22 cm

6 V BATTERY

15 cm³
HELIUM TANK

PRESSURE
SENSOR

PRESSURE
SENSOR

VOLTAGE
REGULATOR
BOARD

SYRINGE
PUMP

PUMP
SERVO

MINIATURE
GC
WAFER

SURGE TANK

GC HOUSING

HIGH
PRESSURE
VALVE

TOP VIEW: BOTTOM LAYER

20 cm

DIGITAL BOARD LEVEL

10 cm

ANALOG BOARD LEVEL

SURGE TANK

COLUMN
HOUSING

INPUT
CHECK
VALVE

SYRINGE
PUMP

GC
WAFER

SOLENOID

FOAM
SUPPORT

INTERNAL VIEW FROM FRONT

Figure 3.7.   LAYOUT OF THE PROTOTYPE MINIATURE GAS ANALYSIS SYSTEM.

21
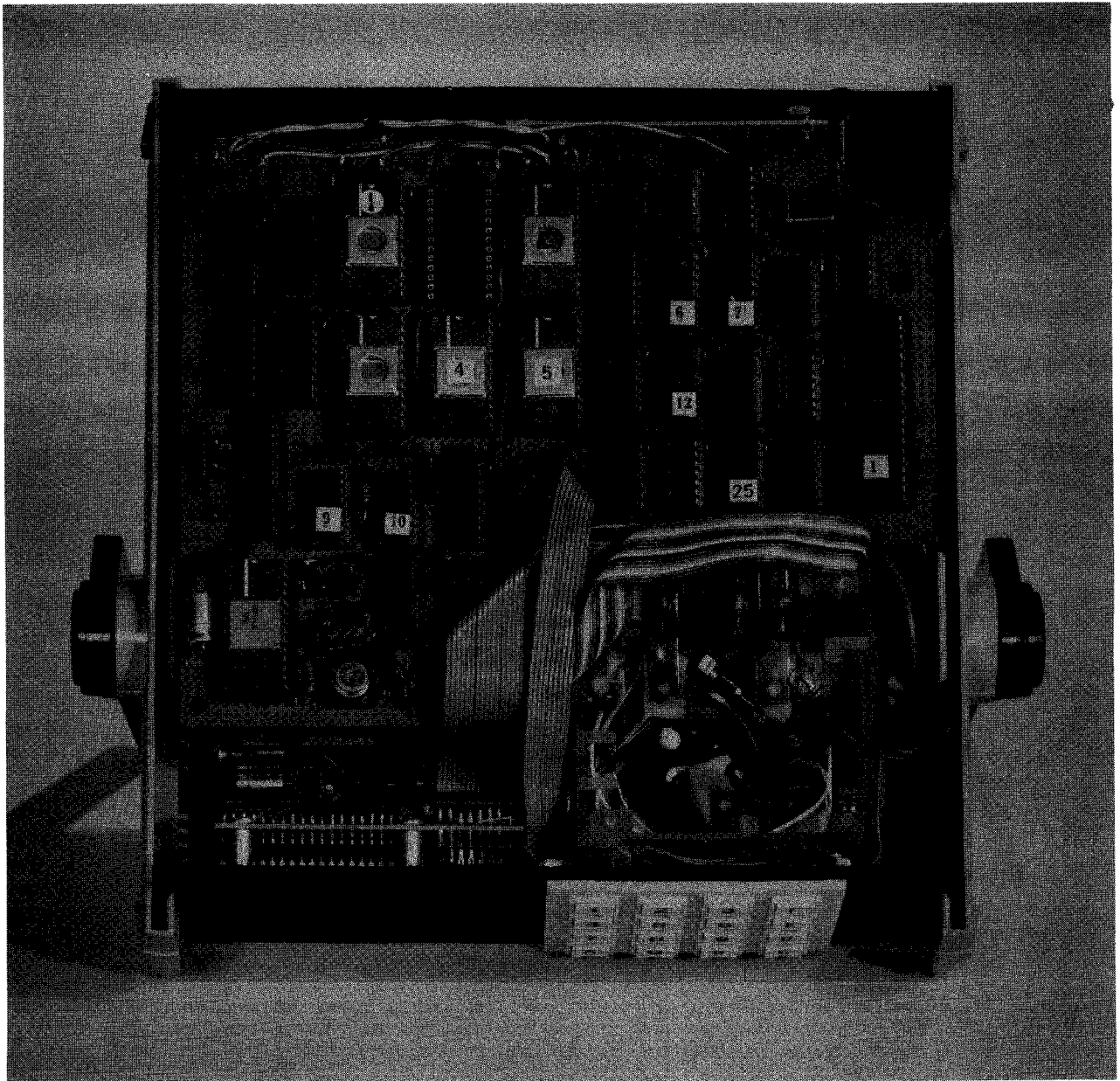
Figure 3.8. PHOTOGRAPH OF THE INTERIOR OF THE PROTOTYPE INSTRUMENT. The
GC is in the lower right and the digital computer board oc-
cupies most of the remaining top layer.

and the electronics, batteries, and carrier gas supply could be carried
on the belt. After the battery and electronics systems are reduced in
size and weight, the total system will be much easier to wear for an 8-
hour shift.

4. PERFORMANCE

The performance of a complicated instrument such as the miniature gas chromatograph is dependent on both the individual performance of the separate elements and the manner in which they are interconnected to form the system. The following section will concentrate on the system performance, with the succeeding sections devoted to the performance of the individual chromatographic, detector and computer sections.

4.1 OVERALL INSTRUMENT PERFORMANCE

The basic measure of performance used for this instrument is the overall system reproducibility, defined here as the ability of the instrument to measure and display the concentration of a standard gaseous sample. Most of the reproducibility tests have used dilutions from commercially available calibrated gas samples of pentane and hexane at original concentrations of 1000 ppm. A large number of analyses are performed on a sample gas, and the mean and standard deviation of the distribution of results are calculated. Since the analyses are performed in less than one minute, a rather large number of essentially independent measurements can be made. The results of a typical test consisting of 50 analyses showed the instrument's measurement of a sample containing both pentane and hexane to have a percent standard deviation of 2.5% for pentane and for hexane, to give a reproducibility at the 95% confidence level of plus or minus 5% at 1000 ppm concentrations. In such a test at approximately room temperature, the pentane retention time is about 3.3 seconds, closely following the air peak, while the hexane at 4.6 seconds is roughly in the middle range of retention times (4 to 8 s) for this instrument.

A series of tests of reproducibility were performed on the prototype instrument. Each test involved taking 50 samples of a gas mixture, and the mean and standard deviation of the concentration results were determined. The gas samples were prepared by successive dilutions of a 1000 ppm standard gas, and due to uncertainties in the dilution process, the dilute gas samples are of unknown absolute accuracy. From the more than 3000 analyses which were performed on the prototype instrument a representative set of 50 consecutive analyses of diluted samples of pentane and hexane at about 50 ppm has been selected and the individual results are shown in Table 4.1. This table lists the computer calculated concentrations of pentane and hexane in ppm and the measured air peak heights in mV from an external oscilloscope. A typical chromatogram from this series is also shown in Figure 4.1. The calculated percent standard deviation for pentane is 3.85% with a mean of 49.7 ppm, and for hexane the mean is 67.9 ppm with a 4.89% standard deviation. The maximum and minimum calculated concentrations are within ± 2 standard deviations of the mean.

23

Table 4.1. Results of reproducibility test.

Run #	Pentane (ppm)	Hexane (ppm)	Air (mV)	Run #	Pentane (ppm)	Hexane (ppm)	Air (mV)
1	51.6	66.1	1962	26	50.7	67.0	1900
	51.6	70.1	1924		50.0	67.4	1924
	46.3	65.9	1902		51.7	69.5	1902
	48.6	66.7	1926		48.5	63.5	1918
5	51.3	61.7	1926	30	49.5	68.7	1942
	48.3	66.3	1932		51.8	66.3	1908
	53.1	68.3	1950		49.8	66.9	1930
	50.7	67.8	1918		48.1	69.1	1924
	49.6	70.0	1918		51.2	73.4	1910
10	48.0	66.8	1912	35	51.1	63.1	1904
	51.8	72.7	1930		48.9	65.4	1912
	46.1	72.0	1922		49.4	65.9	1910
	50.5	68.9	1896		53.0	74.9	1916
	51.6	71.9	1934		49.8	67.0	1916
15	52.1	71.4	1930	40	51.6	67.6	1902
	47.7	65.7	1914		51.2	70.1	1902
	50.6	67.2	1898		50.9	64.3	1908
	50.1	70.7	1918		50.6	64.3	1892
	46.5	67.1	1916		46.3	66.8	1914
20	50.2	67.8	1930	45	47.2	66.1	1914
	47.1	71.6	1926		50.2	62.6	1908
	47.5	62.7	1944		52.7	68.5	1888
	46.2	69.0	1924		48.8	60.3	1908
	48.1	71.5	1932		48.4	65.6	1894
25	51.5	73.9	1910	50	49.7	65.0	1898

Pentane mean: 49.75 ppm
Hexane mean: 67.86 ppm

Retention times:
    Air 2.7 s
    Pentane 3.36 s
    Hexane 4.55 s

Pentane standard deviation: 3.85%
Hexane standard deviation: 4.89%

Column temperature 27°C
OV-101 stationary phase
Helium carrier gas

This use of the percent standard deviation is a valid measure of the re-
producibility of the instrument for single measurements, that is, any
single reading can be expected to be within ± 2 standard deviations of the
mean with a 95% confidence level. When the instrument is used to repeat-
edly sample the atmosphere or a gas sample, the overall reproducibility of
the final time weighted average (TWA) figure will have substantially
smaller percentage error, assuming all other conditions are constant. The
percentage error will theoretically decrease by a factor of $\sqrt{n}$, where n
is the total number of samples. During an 8-hour day, the instrument can
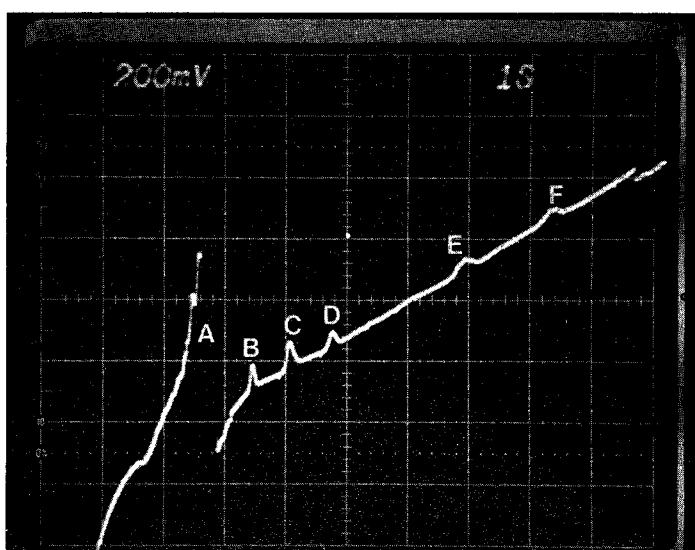
Figure 4.1.   TYPICAL CHROMATOGRAM FROM THE REPRODUCIBILITY TESTS. Peaks
are (A) air, (B) pentane, (C) dichloromethane, (D) hexane,
(E) benzene, and (F) trichloroethane. Sample compounds are
approximately 50 ppm concentrations.

take more than 400 samples, so that the final TWA figures can be expected
to be considerably better than the single reading percent standard devia-
tions. For example, for the pentane results shown in Table 4.1, the mean
for each column of 25 analyses are found to be 49.468 ppm and 50.044 ppm.
These two results have a standard deviation of only 0.82%, which is quite
nearly a factor of $\sqrt{25}$ better than the single measurement error of 3.84%
standard deviation.

The results of a series of tests with pentane, hexane, and carbon tetra-
chloride with concentrations from 10 to 1000 ppm are shown in Figure 4.2.
The reproducibility of pentane is better overall than hexane, for example,
because the retention time of pentane is shorter than that of hexane,
which means that for equal concentrations, the peak height of pentane will
be significantly higher than that of hexane. The increased peak height
improves the signal to noise ratio, which improves reproducibility, es-
pecially at small concentrations. In these tests at room temperature, the
respective retention times for air, pentane, hexane, and CCl_4 were about
2.7, 3.3, 4.6, and 6.0 seconds. Since the pentane peak is only about 500
ms from the air peak, pentane peaks less than 20 ppm are lost in the tail
of the air peak by the present computer program.

The reproducibility of the instrument at larger concentrations of about
2.5% standard deviation is quite acceptable. It is important to identify
the sources of error at the different concentration levels in order to
determine possible future improvements in system performance. The sources
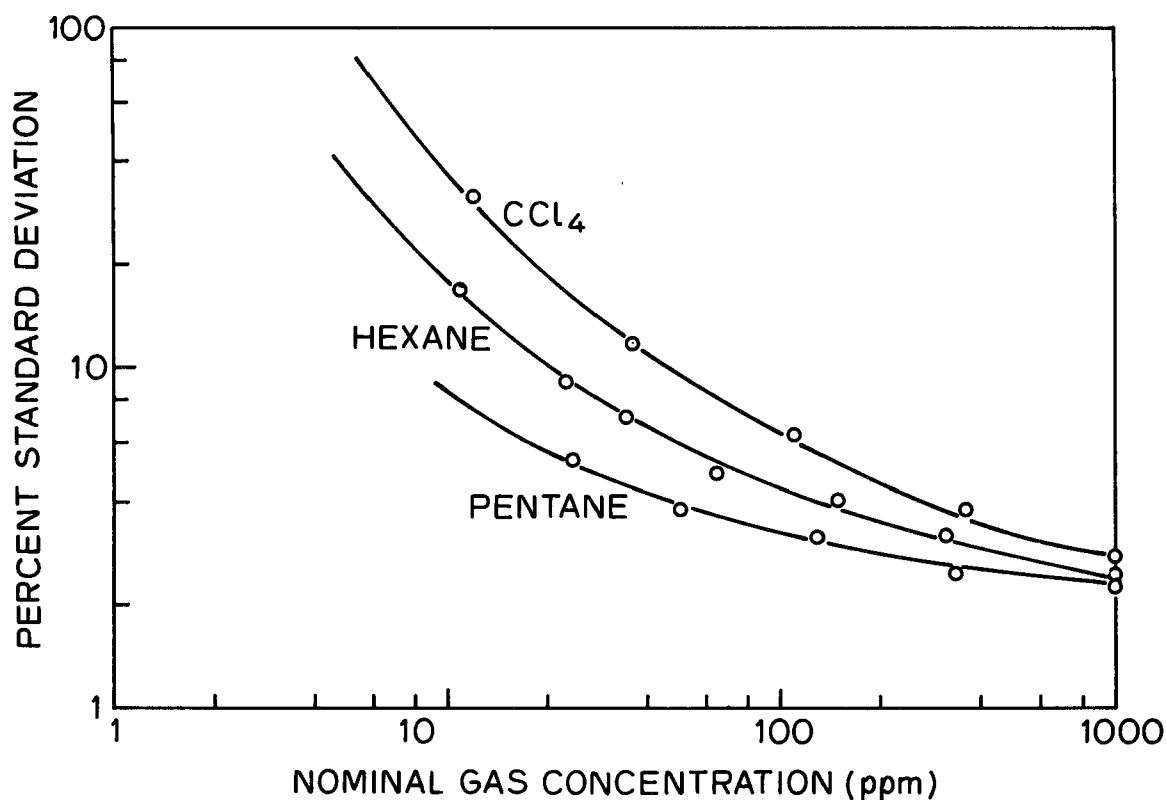
Figure 4.2. SYSTEM REPRODUCIBILITY VS SAMPLE SIZE.

of error fall roughly into four categories, GC system errors, detector noise and nonlinearities, quantization errors in the A/D converter, and errors in the computer algorithms used to compute the peak areas. Each of these sources of error has received some study, and the performance in each area can undoubtedly be improved with additional work.

The GC process itself probably contributes the least amount of uncertainty to the system reproducibility. If identical samples of constant gas concentration are injected at the head of the column, then identical peaks are expected at the output if identical temperature and flow conditions are maintained. Possible sources of error are in the sample collection and injection system, however. Some of these errors, such as slightly different sample injection volumes are taken into account in the final concentration calculation. There are some dead volumes in the sample inlet region which result in a finite rise time of about 4 sampling intervals to reach 95% of a step change in concentration. In the reproducibility test it is assumed that the GC system is basically not responsible for any of the system error.

The GC detector, as discussed in Section 4.3.2, is slightly nonlinear and has some low level noise. In this prototype the detector noise and the analog electronics noise is about 2-μV peak-to-peak, referred to the

26

detector, at nominal operating conditions over a bandwidth of 0.1 to 30 Hz. This detector noise is thought to be due to extremely small flow instabilities in the detector cavity, which causes minute changes in detector operating temperature. This detector noise only becomes important at the lower peak concentrations. The unit is generally operated so that the output peak height, referred to the detector, is about 0.5 to 1.0 μV/ppm for peaks such as hexane and chloroform. In the reproducibility tests, the injection pressure was set so that sufficient sample was injected to obtain about a 2000-mV air peak and a sensitivity of about 0.7 μV/ppm for hexane.

The predominant source of error in the system at lower concentrations is caused by the A/D converter. The present 10-bit A/D converter has a minimum resolution of 5 mV. Under the conditions of the reproducibility test, a 20 ppm hexane peak is 70 mV, which is about 14 A/D levels in amplitude. This lack of amplitude resolution introduces significant error in the peak area calculation.

When measuring small gas concentrations, it is possible to improve reproducibility by a factor of about 2 in the sub-10 to 50 ppm range by increasing the size of the peaks by injecting a sample at higher injection pressure. This increases the amplitude of the peaks, which improves the signal to noise (S/N) ratio. The only disadvantage of this procedure is that a 1000 ppm sample of, for example, pentane would be so large as to be out of the dynamic range of the A/D converter. Thus, at higher injection pressures it would not be possible to simultaneously measure a 1000 ppm hexane peak and a 10 ppm CCl_4 peak.

Peaks in the 20 ppm range are still well above the detector and electronics noise level so the reproducibility at these levels could be improved by increasing the gain of the amplifier or by increasing the resolution of the A/D converter. The amplifier gain has been selected such that a 1000 ppm pentane peak is just in the maximum range of the converter. It would be possible to change the gain of the amplifier during the chromatograph, but this would introduce additional complications in the computer program, which would probably unacceptably slow down the program, and would further reduce the sampling rate. A 12-bit A/D converter is presently being tested and is most likely the quickest way to achieve better performance, and when faster, low power computers become available, the program can be modified to handle amplifier gain changes.

It appears that the main source of inaccuracy in the computer system is the finite sampling rate. The computer has only enough time to take about 30 samples during the time equivalent to two standard deviations of the roughly gaussian output peaks. This causes imprecision in the determination of the peak standard deviation which is used to calculate the peak area, which is further used to determine the peak concentration. There are two ways to reduce this error. One is to sample faster, which would require faster and more sophisticated computers, and the other is to use an additional interpolating filter to achieve higher precision than the sampling frequency allows. Both approaches may be used in more advanced versions of the instrument.

4.1.1 Analog Electronics Performance

The computer system, since it is digital, is immune to temperature and battery voltage changes, as long as they remain within the operating range of the devices. The analog electronics, however, is subject to temperature and power supply variations. Most of these variations can be minimized by appropriate circuit design, and the use of resistors and capacitors with inherently low temperature coefficients. The primary reference element in the analog electronics is a voltage source which is stable to within 0.08% over the operating temperature range of 0 to 45°C.

The reduced results of the analog electronics test are shown in Table 4.2. This test measured the changes over a temperature range of from 25 to 50°C and over the maximum voltage range of the two batteries of +5 to +7 V and −14 to −10 V. The two individual effects are listed along with the total extreme over both temperature and voltage. The portions of the circuit measured are the most important ones for the analytical performance of the

Table 4.2. Analog electronics performance.

Circuit	Drift over Temp 25°C to 50°C	Drift over Supply −14,7 to −10,5	Total Extreme T and V
Thermistor amp equiv. drift	0.064°C	0.034°C	0.10°C
Detector amp zero drift	2.2 mV	0.34 mV	4.6 mV
Pressure output zero drift	0.58 psi	0.07 psi	0.70 psi
Pressure output 30 psi	0.17%	0.37%	0.37%
Swept time number 10 seconds	0.63%	0.72%	1.6%
Detector current	1.08%	0.65%	1.65%

instrument. The thermistor amplifier error is the output voltage error due to the reference and amplifier converted to an equivalent temperature measurement error. The detector amplifier zero drift is the total output voltage change of the x1 amplifier with a metal film resistor in place of the detector. This 4.6-mV total change is less than 1 A/D level and includes the effects of current source changes on the input bridge, the temperature change of the detector reference resistor, and the x1 amplifier drift. Even though this change is small, after an additional gain of 5000 the drift would be considerable. The high gain amplifier is zeroed before each chromatogram to reduce the effect of these drifts on the high gain output. If the instrument is subjected to a 20°C step change in temperature, the resulting high gain output drift is about 1 V during a chromatogram. The pressure errors include the temperature effects of the pressure

28

sensors along with the bridge driving voltage and the transducer amplifiers. The swept time error is the change in the number of clock pulses generated over a 10 second period by the swept time circuits. The 1.6% total error corresponds to less than a standard deviation of one of the output peaks. The relatively large (1.65%) total error in detector current is of little importance, since the detector sensitivity is changed little by this difference, and the concentration calculation performed by the computer is concerned only with the relative sizes of the air and sample peaks, so sensitivity changes cancel when the ratio is taken.

4.2 GC COLUMN PERFORMANCE

The performance of any GC column is determined by a myriad of parameters, including the thermodynamic properties of gases and liquids, and the geometry of the column and its effects on gas flow. In general, the most important factors are the stationary phase used and the geometry of the GC column. Since the start of gas chromatography in the 1950's, there have been numerous attempts to provide a complete theoretical description of the gas chromatography process. The geometry of the miniature chromatograph is sufficiently similar to that of conventional instruments that the GC theory can be used to provide clues to help optimize the analytical performance of the instrument. Unfortunately, the mathematical descriptions of the actions of the GC linings do not indicate how to actually line a column to produce maximally efficient linings. The lining techniques must be separately developed for the modified geometry of the miniature GC, and the theory can then be used to optimize the size of the columns to perform specific separations.

4.2.1 Column Linings

The stationary phases used thus far in the miniature capillary columns have been the same substances as those used in conventional gas chromatography. Modified lining techniques have been developed which achieve reproducible, uniform distributions of the stationary phases on the column walls. Most of the separations performed with the miniature capillary columns were achieved with a silicone oil, OV-101, as the stationary phase. The following sections describe the column treatment and lining procedure for the OV-101 liquid phase.

Column Pretreatment--
The construction of the integrated capillary column is such that the capillary bottom and side walls are silicon while the top plate is Pyrex glass; however, the silicon surface is coated with a layer of silicon dioxide (SiO_2) several tens of Angstroms thick which is formed during the anodic bonding process. The SiO_2 and glass surfaces are naturally covered with a high density of silyl ether and hydroxyl groups. Treatment of these surfaces with an aqueous solution of a strong acid (e.g. concentrated HCl) converts many of the surface ethers into hydroxyl groups.

$$Si{\diagdown}\atop{Si\diagup} O + H_2O \xrightarrow{\quad H+ \quad} \begin{matrix} Si-OH \\ \\ Si-OH \end{matrix}$$

29
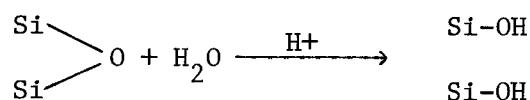
These surface hydroxyl groups will react with organosilane compounds of the form $RSiX_3$ or R_3SiX (where R is an alkyl group and X is either a chloride or an alkoxide group) to form a Si-O-Si linkage between the silicon and the silane as

$$Si-OH + R_3SiX \rightarrow Si-O-\overset{\displaystyle R}{\underset{\displaystyle R}{Si}}-R + HX$$
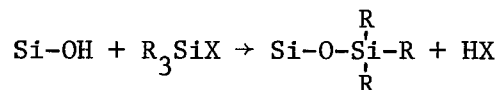
We have employed this chemistry to react trimethylchlorosilane $(CH_3)_3 SiCl$ with the column surface. The reaction is carried out by forcing the undiluted silane through the column for about 10 min at 70°C. The capillary is then washed with water and methanol and blown dry. This procedure serves to convert the OH groups which populate the surface of the column and to provide a monomolecular layer to which the stationary phase can adhere.

Dynamic Column Lining--
The liquid stationary phase can be applied to the miniature capillary walls by means of a conventional dynamic coating procedure [3]. The OV-101 liquid is dissolved in a very volatile solvent such as chloroform, and a plug of the mixture is forced through the column. If the speed of the moving plug is kept constant, a uniformly thick layer of OV-101 is left on the column walls. The approximate thickness (t) of the layer is given by

$$t = \left(\frac{C}{100}\right)\left(\frac{r}{2}\right) \sqrt{\frac{\mu\eta}{\gamma}}$$

where C is the concentration of the solution (%v/v), r is the radius of curvature of the capillary tube, μ is the average velocity of the plug of lining solution, η is the solution's viscosity, and γ is its surface tension.

Although this lining procedure is common practice with conventional capillary GC columns, it is less than ideal for the miniature capillaries since they have extremely smooth surfaces and nonconstant radii of curvature. The resulting distribution of stationary phase appears to be nonuniform both across the width of the capillary channel and along its length. The lining distribution is unstable with time and the OV-101 bleeds out of the column.

The distribution and performance of the column lining can be significantly improved with the addition of a small percentage of 7-10 Å SiO_2 particles into the OV-101 liquid phase. These particles tend to increase the stability of the thin liquid layer and result in greater surface area of liquid phase per unit length of column, an attribute which increases the column's ability to separate gases.

All of the miniature capillary columns which are fabricated now include SiO_2 particles in the liquid stationary phase. A column lined with OV-101

and SiO_2 particles was operated with constantly flowing carrier gas for more than 6 months. No attempt was made to condition the column, and numerous temperature cycles were performed, but the relative retention times of the peaks changed less than 10% over the length of the test, and no detectable amount of column lining was blown into the detector channel.

Static Column Lining—
With the miniature capillary column as well as with conventional columns, the static coating procedure [4] is replacing the dynamic method because it yields more reproducible and uniform stationary phase distributions. The OV-101 liquid is dissolved in chloroform along with SiO_2 particles and the capillary is totally filled with the mixture. The output end of the capillary is then sealed off and the miniature GC column is put in a vacuum chamber at less than 1 Torr pressure. The chloroform in the capillary evaporates slowly from the head of the column leaving the OV-101/SiO_2 residue coating the capillary walls. The evaporation rate is slow and constant and all of the OV-101 remains in the column. This procedure gives very uniform lining distributions in which the exact weight of liquid phase per unit length of column is known.

4.2.2 GC Separations

One of the important features of the miniature gas chromatograph is its very, rapid separation of the gases of interest. As a simple example of its capabilities, an oscilloscope photograph of the amplified detector output, or chromatogram, is shown in Figure 4.3. The sample gas consisted of a mixture of nitrogen, pentane, and hexane vapors and was injected at time zero. The nitrogen has no affinity for the OV-101 column lining so
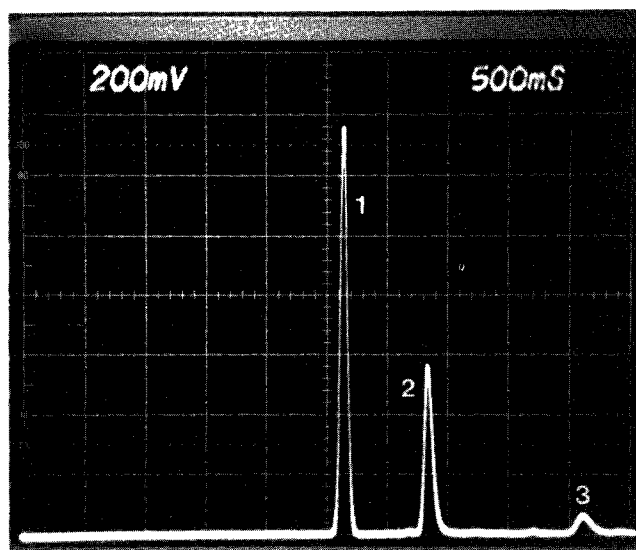
Fifugre 4.3. OSCILLOSCOPE PHOTOGRAPH OF THE AMPLIFIED DETECTOR OUTPUT OR CHROMATOGRAM. The sample was injected at the beginning of the sweep. The peaks are (1) nitrogen, (2) n-pentane, and (3) n-hexane.

31

it emerged from the column after 2.6 seconds, a time determined solely by the helium carrier gas velocity. The finite base width of the nitrogen peak ("air peak") is caused by gaseous diffusion of the nitrogen in the carrier gas, since the injected peak was only 5.0-ms wide and there are no appreciable mixing or detector time constants. The next peak at about 3.3 seconds is the pentane, followed at 4.6 seconds by the hexane. The increased retention times are due to the times spent by the pentane and hexane adsorbed on the column lining, and the increased base widths of these peaks are due both to gaseous diffusion and diffusion of the species in the column lining. It is preferable to keep the peak spreading to a minimum, since this will facilitate the separation of more components of a mixture and will maximize the peak height which increases the signal to noise ratio of the detector. The complete separation was performed in less than 5 seconds, which is significantly less than the several minutes which a conventional GC system might take to give the same separation.

Figure 4.4 shows another output chromatogram using OV-101 as the stationary phase. This example shows the ability of the device to separate very similar branched and straight chain hydrocarbons as well as chlorinated hydrocarbons. Again, the relatively short length of the miniature capillary column (1.5 meters) enabled the separation to be performed in less than 10 seconds. The analysis time is shorter than a typical conventional GC, but the separation of these closely related chemicals which was achieved by the miniature GC is not as good as could be achieved with a standard column. By applying capillary GC theory the separating power of the miniature GC can be characterized.
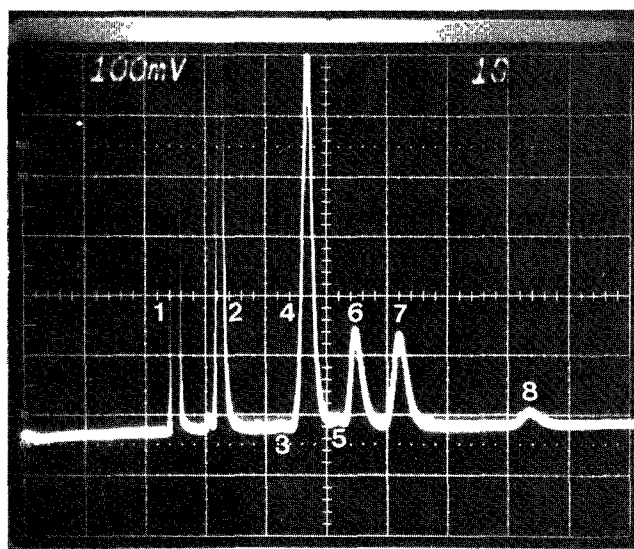
Figure 4.4. MINIATURE GC CHROMATOGRAM USING OV-101 STATIONARY PHASE. Peak (1) nitrogen, (2) n-pentane, (3) 3-methylpentane, (4) n-hexane and chloroform, (5) 2,4-dimethylpentane, (6) 111-trichloroethane, (7) cyclohexane, and (8) n-heptane.

32

The sketch of an idealized chromatogram shown in Figure 4.5 defines the parameters which characterize an output peak. The retention times from sample injection to the maximum of each peak for the unretained air peak and the sample peak are t_M and t_R respectively. An important measure of the operation of the column is the length of time that the sample is retained by the stationary phase. This is the adjusted retention time t'_R, given by $t'_R = t_R - t_M$. For a gaussian peak with standard deviation σ, the peak basewidth is defined as $W = 4\sigma$.
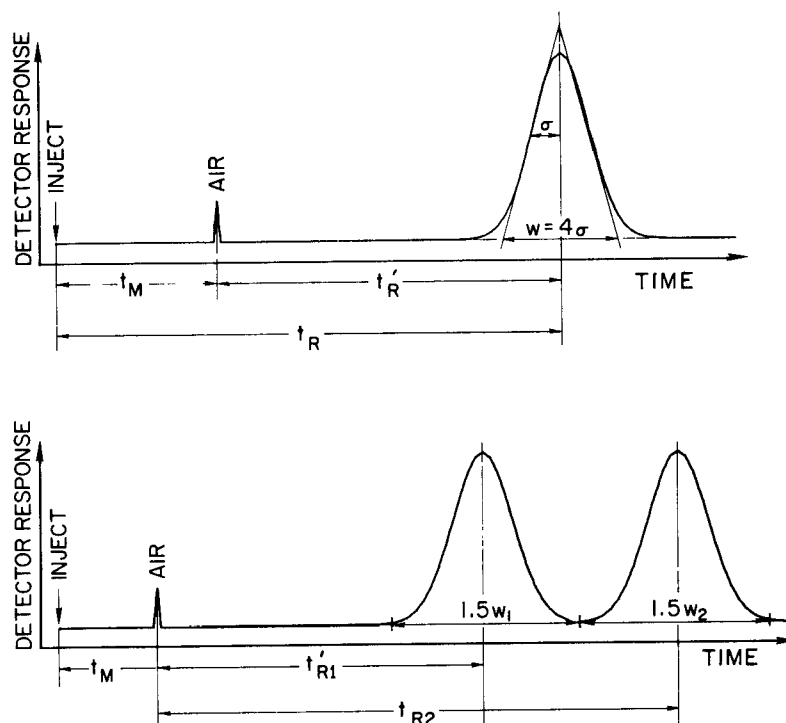
Figure 4.5. IDEALIZED CHROMATOGRAM SHOWING RETENTION TIMES AND PEAK WIDTHS.

One practical measure of column efficiency is the effective number of theoretical plates (N) in the column,

$$N = 16 \left(\frac{t'_R}{W}\right)^2 \tag{1}$$

It is desirable for N to be large, indicating a well retained yet very narrow peak. The number of effective plates calculated for the peaks in Figure 4.4 ranges from 385 for peak #2 to 2300 for peak #8. For 30-m long and efficient standard capillary columns, the number of effective plates typically ranges between 10,000 and 100,000. The improvement in performance of the conventional column is due to its greater length and the superiority of its stationary phase distribution.

33

The utility of the number of effective plates lies in its ability to predict if a column is efficient enough to resolve two peaks whose adjusted retention times t'_{R1} and t'_{R2} are very close. The standard measure of resolution of two peaks is defined as

$$R = \frac{t'_{R2} - t'_{R1}}{(W_1 + W_2)/2} \tag{2}$$

A resolution value of $R = 1.5$ results in peaks separated as shown in Figure 4.5B. The number of effective plates, N, needed for a column to separate two peaks with a resolution of $R = 1.5$ can be determined from

$$N = 32 \left(\frac{\alpha}{\alpha - 1}\right)^2 \tag{3}$$

where $\qquad \alpha = \dfrac{t'_{R2}}{t'_{R1}}$

As an example, consider peak #4 of Figure 4.4. This peak is really two unresolved peaks of chloroform and hexane for which $\alpha = 1.05$. Equation (3) predicts that the column would need N = 14,122 plates to just separate those two vapors. Since N was only 1067 plates for this particular column, those two vapors were not separated and thus appeared as only a single peak.

The ability of the miniature capillary column to separate peaks is determined by the stationary phase, the column geometry, and the column operating conditions. The current columns 1.5-m long by 40-μm by 175-μm wide and lined with OV-101, are only about 20% efficient. That is, the columns exhibit only 20% of the maximum number of theoretical plates possible for a column with those dimensions. Thus, improvements in the stationary phase composition and lining techniques should result in a significant improvement in column performance. Once the stationary phases have been improved, the dimensions of the capillary columns can be optimized for given applications and specific separations.

4.2.3 Optimization of the GC Column

The number of effective theoretical plates that a column possesses for any gas is related to another parameter, the plate height (H) by

$$H = \frac{L}{N} \left(\frac{k}{1 + k}\right)^2$$

where L is the column length and k is the partition ratio for a gas of interest and is given by

34

$$k = \frac{t_R'}{t_M}$$

The plate height of an open-tubular capillary column with rectangular cross-section has been related to the column parameters by Golay [5] as

$$H = \frac{B}{u} + (C_\ell + C_g)u \qquad (4)$$

where

$$B = 2D_g$$

$$C_\ell = \frac{2k^3 z_0^2}{3(1 + k)^2 K^2 D_\ell} \qquad (5)$$

$$C_g = \frac{4\left[(1 + 9k + 51k^2)/2\right]z_0^2}{105(1 + k)^2 D_g} \qquad (6)$$

and

z_0 = 1/2 of the etched column depth

u = carrier gas velocity

D_g = diffusion coefficient of solute vapor in carrier gas

D_ℓ = diffusion coefficient of solute vapor in liquid stationary phase

The partition <u>ratio</u> k used in the above equations is a function of the column height and width. It is related to a more fundamental parameter, the partition <u>coefficient</u> K, by the equation*

---

*The partition coefficient is defined as the concentration of solute vapor in the stationary phase divided by the concentration in the mobile phase. It is only a function of the thermodynamic properties of the solute vapor and the stationary phase. Its exponential dependence on temperature makes it the most temperature-dependent parameter, and thus facilitates the control of column performance with simple temperature adjustments.

$$k = \frac{d(2Z_0 + Y)}{Z_0 Y} K \qquad (7)$$

where

    d = thickness of the layer of liquid phase lining the column

    Y = column width

The B/u term in Equation (4) accounts for peak spreading due to longitudinal diffusion of vapor molecules (diffusion parallel to the column axis). Longitudinal diffusion occurs only while the vapor molecules are in the mobile phase and can be characterized by a diffusion coefficient D_g for the specific vapor in a specific carrier gas.

The C_g and C_ℓ terms can be regarded as the "resistance to mass transfer" of the solute vapor in the mobile and stationary phases, respectively. They represent the departure from the ideal condition of instantaneous equilibrium between the vapor in the gas and liquid phases. C_g is associated specifically with the parabolic carrier gas profile across the column's vertical dimensions. The faster moving vapor molecules in the center of the gas stream take longer to diffuse to the stationary phase than do their slower counterparts near the column walls. C_g can be reduced by reducing the column depth (thus shortening the diffusion path for any vapor molecule) or by increasing D_g (speeding up the rate of diffusion).

The C_ℓ term accounts for the diffusion of vapor molecules into the liquid stationary phase. Once a vapor molecule impinges upon the liquid surface, it tends to migrate into the liquid phase as the vapor concentration increases locally in the mobile phase. As the vapor peak passes by and the mobile phase concentration decreases, the process is reversed, and the vapor molecules in the liquid diffuse back to the surface and transfer to the gas stream. The C_ℓ term can be reduced by increasing the vapor diffusion rate through the liquid phase (increasing D_ℓ) or by reducing the liquid layer thickness d.

Since the Equation (4) for plate height contains the carrier gas velocity in both the numerator and denominator, it can be minimized with respect to u. Such an optimization yields

$$u_{opt} = \sqrt{\frac{B}{C_g + C_1}}$$

$$H_{opt} = 2\sqrt{B(C_g + C_1)}$$

A Golay plot of H as a function of carrier velocity can be generated
experimentally, and a typical plot for a miniature column is shown in
Figure 4.6. The values of B, C_g, and C_ℓ as well as the optimum carrier
velocity can be derived from this plot. Unfortunately, almost all of
the terms of Equation (4) are functions of column geometry and partition
ratio parameters; however by assuming typical column operating conditions
and plotting Equation (4) as a function of a specific column parameter,
some insight can be gained into that parameter's effect on the operation
of the column.
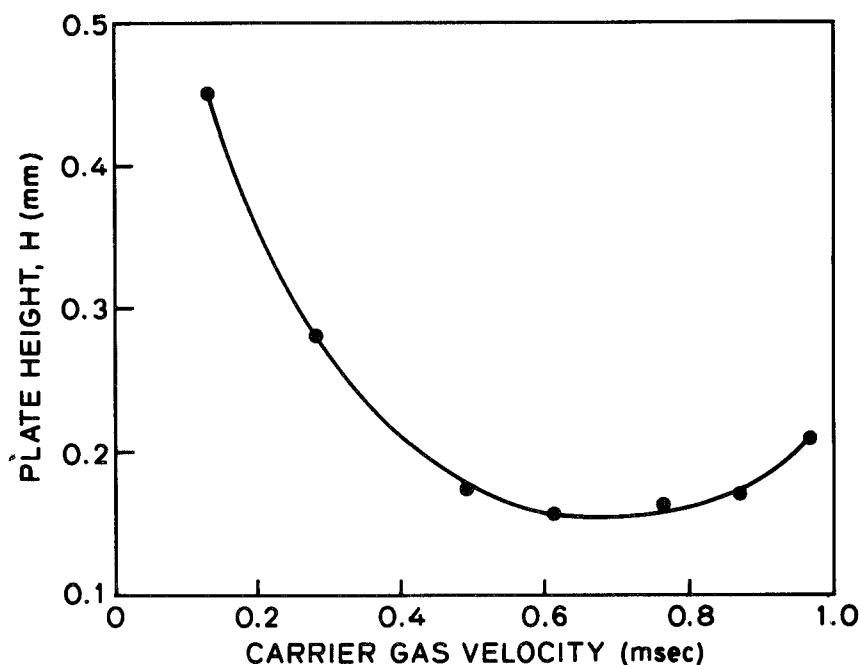
Figure 4.6.   GOLAY PLOT OF MINIATURE CHROMATOGRAPHIC COLUMN WITH OV-101
              COLUMN LINING.

The most signficant geometrical feature of the miniature capillary column
is its roughly rectangular cross section with very shallow depth (Z). The
calculated values of H_{opt} and N_{opt} are plotted in Figure 4.7 as a function
of column depth. The carrier gas velocity required to achieve these opti-
mum values is plotted in Figure 4.8 as a function of column depth. It is
obvious from Figure 4.7 that the best column performance (largest number
of effective plates, N) is realized as the etched column depth is decreased.
However, the price to be paid for increasing the column efficiency by re-
ducing its etched depth is the much higher pressure drop across the column
which is required to achieve the optimum carrier gas velocity. Given a
maximum operating pressure, Equation (4) can once again be used to show
how N varies with column depth. Such curves are plotted in Figure 4.9 for
several values of maximum carrier pressure. Clearly there is an optimum
column depth for each value of carrier pressure.

37
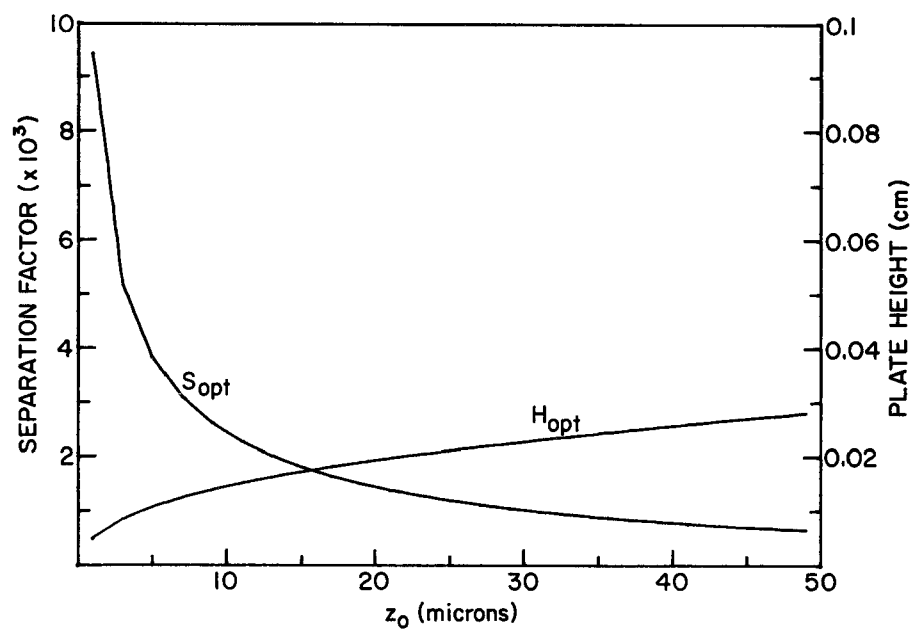
Figure 4.7.   OPTIMUM PLATE HEIGHT AND SEPARATION FACTOR AS FUNCTIONS
OF COLUMN DEPTH (Z_0).
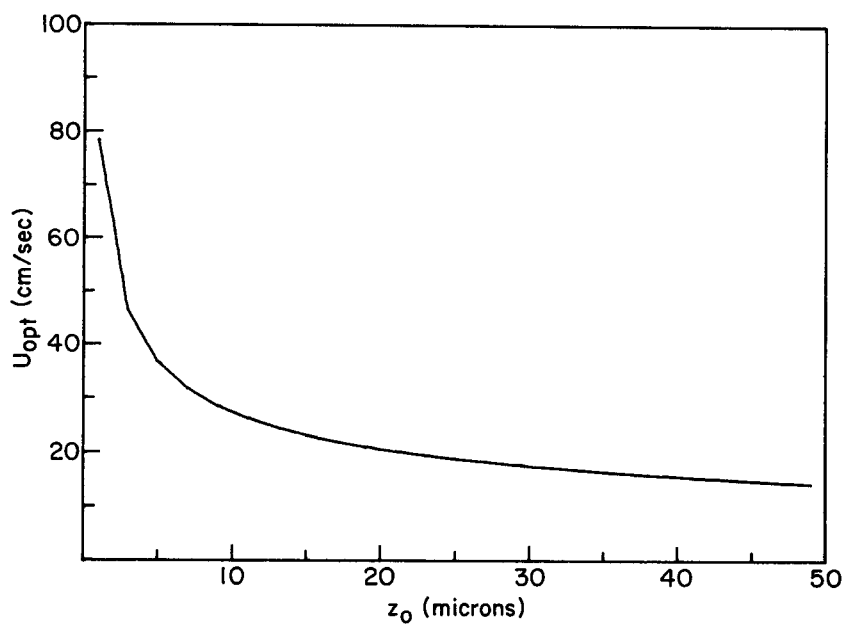
Figure 4.8.   OPTIMUM CARRIER GAS VELOCITY AS A FUNCTION OF Z_0.

38
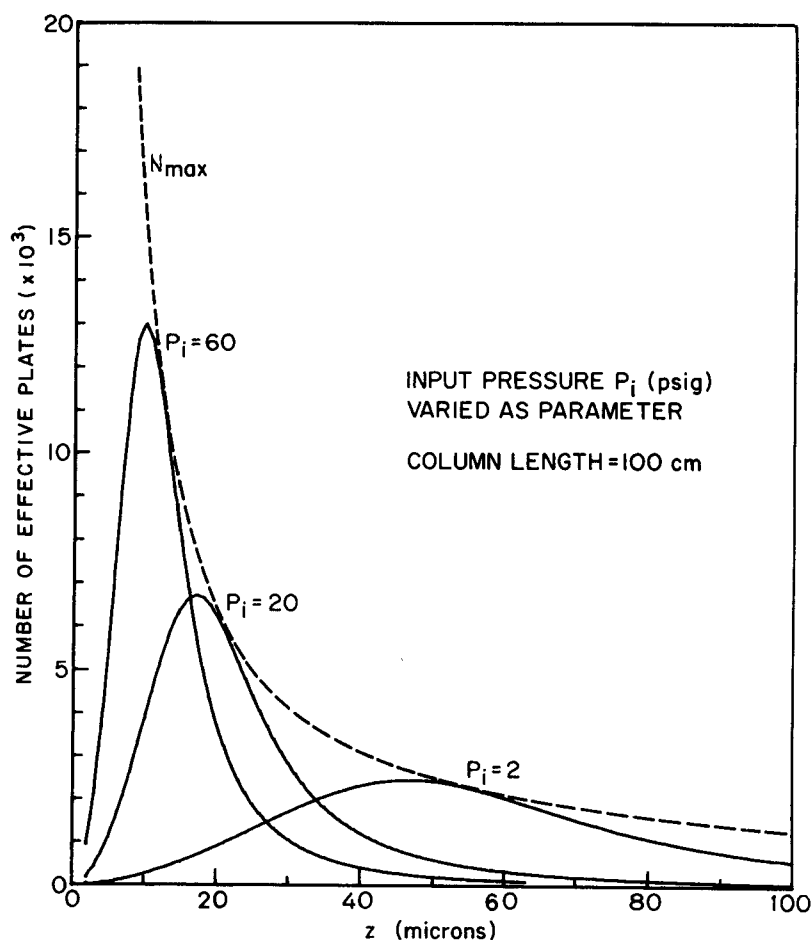
Figure 4.9. NUMBER OF EFFECTIVE PLATES AS A FUNCTION OF MAXIMUM ALLOWABLE
CARRIER GAS PRESSURE AND ETCHED DEPTH.

The preceding example illustrates how one of the many parameters which con-
trol the operation of the miniature capillary column can be optimized to
increase the efficiency of the column. When such analyses are performed
for the other column parameters, the following guidelines are suggested for
optimizing the design of the miniature column with a specific stationary
phase for the separation of a known group of sample vapors.

(1) The maximum allowable carrier gas pressure should be used.
As shown in Figure 4.9, the peak value of the number of ef-
fective plates increases with input pressure.

(2) The column should be optimized for the separation of the
vapors with the smallest retention times or for the most
difficult separation.

(3) The column length should be as long as possible if the maxi-
mum separation is desired.

(4) Once the values of the partition coefficient, column length, and carrier pressure are known, a plot of Equation (4) will indicate the column depth which maximizes the separating power of the column.

Such an optimization of the miniature capillary column must be tailored to fit many other requirements imposed by the rest of the instrument systems. For example, the column dimensions and the carrier gas velocity determine the rate of consumption of carrier gas and thus influence the size of the helium supply tank. Long columns are desirable to perform difficult separations, yet the resulting analysis time may be prohibitively long. Very short columns for rapid separations are too fast for the computer to keep up with in real time, and thin column linings require very small sample injections which may limit system detectivity. Many such trade-offs exist, making system optimizations a difficult task.

The miniature GC columns which are currently in use are 1.5-m in length with 40-μm x 175-μm cross sections. There has been no comprehensive effort to optimize the geometry of these columns since the stationary phase distribution and performance are not under good control. The choice of some of the column dimensions and operating parameters has been dictated by reliable valve operating pressures, desired anslysis times, and by computer speed.

The column length of 1.5-m was arbitrarily chosen at approximately half of the maximum length that we can currently fabricate. The 40-μm column depth gives air peak retention times of 1 to 3 seconds over carrier pressures of 30 to 10 psig. The Golay plot shown in Figure 4.6 indicates that carrier gas velocities between 61 and 87 cm/s yield the minimum plate height and hence the best column performance for the stationary phase distribution which is currently achieved. The velocity of 61 cm/s, which corresponds to a helium carrier gas pressure of 19 psig, was chosen so that the resulting air peaks and little-retained gas peaks would have base widths of at least 130 ms. Such peaks are of the minimum width which can be adequately sampled by the microcomputer.

The nonpolar columns which are currently used are only partially optimized as described above, but the optimization process will continue as better stationary phases, detectors, and computer hardware and software systems are developed.

4.2.4 Temperature Dependence

The retention time of a sample vapor in a GC column is a strong function of the column temperature. For this reason, conventional chromatographs typically maintain an elevated column temperature constant to within 1°C or better, or they utilize temperature programming to facilitate certain separations. In the portable instrument there is insufficient battery power to run a controlled-temperature oven, so the capillary column operates at approximately room temperature. Since room temperature varies roughly between 0 and 45°C, the computer must be able to predict the retention times of all peaks of interest over this temperature range.

The temperature dependence of retention follows directly from the exponential relation of equilbria in phase transformations such as vaporization to which the partitioning of a solute between gas and liquid phases is closely related. The equilibrium partition coefficient K is given by

$$K = C \exp \left(\frac{-\Delta H_s}{RT} \right)$$

where

    C is a constant

    ΔH_s is the heat of solution

    R is the gas constant

    T is the absolute temperature

The solution process is usually exothermic (ΔH_s is negative), thus increasing T decreases K.

Over the limited temperature range at which the column operates, ΔH_s is assumed to be constant and the partition ratio k is found from Equation (7) to be of the form

$$k = A \exp \left(\frac{-\Delta H_s}{RT} \right)$$

The constants A and ΔH_s can be determined experimentally for each gas on a miniature capillary column by performing separations over the temperature range and fitting an exponential curve to the data. Figure 4.10 shows the results of such a procedure for chloroform and methylene chloride on an OV-101 capillary column.

To predict the retention time of a given gas, the computer only has to measure the column temperature, insert the appropriate values of A and ΔH_s, and determine the partition ratio k. Then using the air peak retention time (t_M) from the previous chromatogram, the gas retention time is calculated as

$$t_R = t_M (1 + k)$$

4.3 DETECTOR PERFORMANCE

A metal film thermal conductivity detector has been chosen for use in the integrated gas chromatograph. This device was chosen for its compatibility
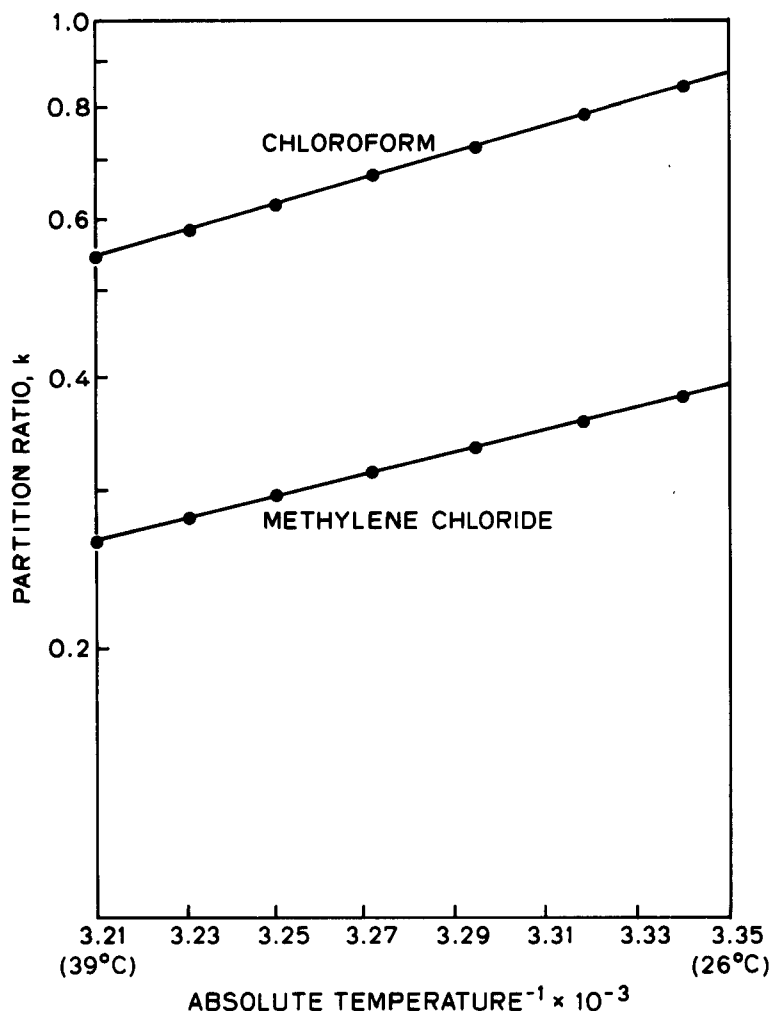
Figure 4.10. PARTITION RATIO AS A FUNCTION OF 1/T FOR CHLOROFORM AND METHYLENE CHLORIDE.

with the miniature system, ease in fabrication, generality of response, and ruggedness. In the many months of testing it has been shown to be a consistent performer.

4.3.1 Comparison with Other Detectors

There are a number of different types of detectors used in gas chromato-graphy. They measure one of a wide variety of physical parameters of the output gas stream. Of the detectors with relatively general response, the most commonly used are flame ionization detectors and thermal conductivity detectors. Lately photoionization detectors have been shown to be a general purpose detector with good analytical performance. The ionization detectors are typically known for their high sensitivity to hydrocarbons, and the thermal conductivity detectors are used for applications where their generality of response to nonhydrocarbons is important.

The flame ionization detector works by introducing hydrogen in the output gas stream of the chromatograph. The resulting gas mixture is then ignited

42

in a burner, the hydrocarbons in the output gas stream are burned, and a small percentage of the combustion products become ionized. These ions are collected by electrodes and the current between the electrodes is integrated to determine the mass of sample in an output peak. The ability of a flame ionization detector to measure small concentrations is due to its low background current and the ability of electronic systems to measure small currents.

The most important property of a detector for many applications is its detectivity. Since ionization detectors are basically mass sensitive instruments, their response is generally given in coulombs/gram and minimum detectable quantities in grams. Thermal conductivity detectors are concentration sensitive devices where the minimum detectable sample is usually given in parts-per-million. The miniature gas chromatograph has some unusual properties due to its small size and small gas flows. It places stringent requirements on the detector. One aspect of these requirements is the small sample that the detector system will be required to measure. In order not to overload the capillary column, the injected sample must be kept very small, in most cases about 10 nl of gas. For many substances, it is desired to measure concentrations below the 5 ppm level. For gases with molecular weights around pentane, 5 ppm of 10 nl of injected gas represents only about 150×10^{-15} grams (150 fg). Because of the gas flow rate of about 4-μl/s out of the column and the narrow peak widths of less than 100 ms, the absolute maximum detector volume cannot exceed 20 nl, without serious peak broadening due to dilution in the detector volume. Thus for a column with chromatographic efficiency similar to that of the prototype, the maximum detector dimensions are 100 μm x 200 μm x 1000 μm. If a shorter column is used or if more efficient linings are developed, the maximum allowable detector volume would be reduced by a corresponding factor.

For purposes of comparison, the detectivity of a high quality flame ionization detector is 18 pg [6] of, in this case, propane, some two orders of magnitude larger than needed for the integrated gas chromatograph. Even a photoionization detector, which is reported [7] to have significantly better detectivity than the flame, can see no less than 6 pg of benzene, again almost two orders of magnitude larger than is needed. These figures were found by injecting quite large volume samples into short, packed columns. In the photoionization case, 5 ml of 0.3 ppb benzene was used. Even though the concentration of this sample is very low, the total mass of the sample is still quite high, and the volume of injected sample is equal to the total carrier gas flow for the miniature system for 25 minutes. These detectivity problems, coupled with the difficulties associated with trying to fabricate an ionization detector in a region a few hundred micrometers across, have limited the feasibility of making a miniature ionization detector.

Conventional thermal conductivity detectors have not been known for their good detectivities. A Varian 3700 TCD can achieve sample detectivities of 1 ng [8], about four orders of magnitude larger than needed for the miniature system. The Varian system also has a minimum detectable peak concentration of about 200 ppb at the detector. The important property of thermal conductivity detectors is that they are concentration sensitive

43

detectors, that is, the output signal is proportional to the concentration
of sample gas in the output gas stream. If the dimensions of the detector
are reduced, the sensitivity of the detector is not greatly affected.
This allows a thermal conductivity detector to be made on the size scale
required for the integrated GC without a penalty for the small dimensions
involved. The detector retains the concentration performance of the larger
detectors, and since the detector volume is so much smaller, the mass
detectivity is reduced to very small levels. The integrated TCD described
below is capable of detecting below 150 fg of injected pentane and has a
detector volume of less than 1 nl.

4.3.2 Detector Operation

The nickel film integrated TCD used with the miniature gas chromatograph
is shown again in Figure 4.11. A nickel film was chosen as the sensing
element because of its relatively high temperature coefficient of resis-
tivity (TCR), moderately high melting point, ease of deposition and
selective removal, and relative inertness. Most larger TCD's use tungsten
or tungsten alloys for the sensing element which have about the same TCR,
a higher melting point, but more difficult deposition than nickel. The
structure and fabrication sequence used for the detectors can accommodate
a wide variety of metals as sensors; nickel has performed adequately in
the initial tests.

There are a number of ways to heat the sensor. In a self-heated system
the choices are among the electrical circuit configurations used to drive
the detector. The three most common are the bridge, constant current, or
constant temperature. Each different drive configuration produces dif-
ferent sensitivity, thermal time constants, temperature extremes, linearity
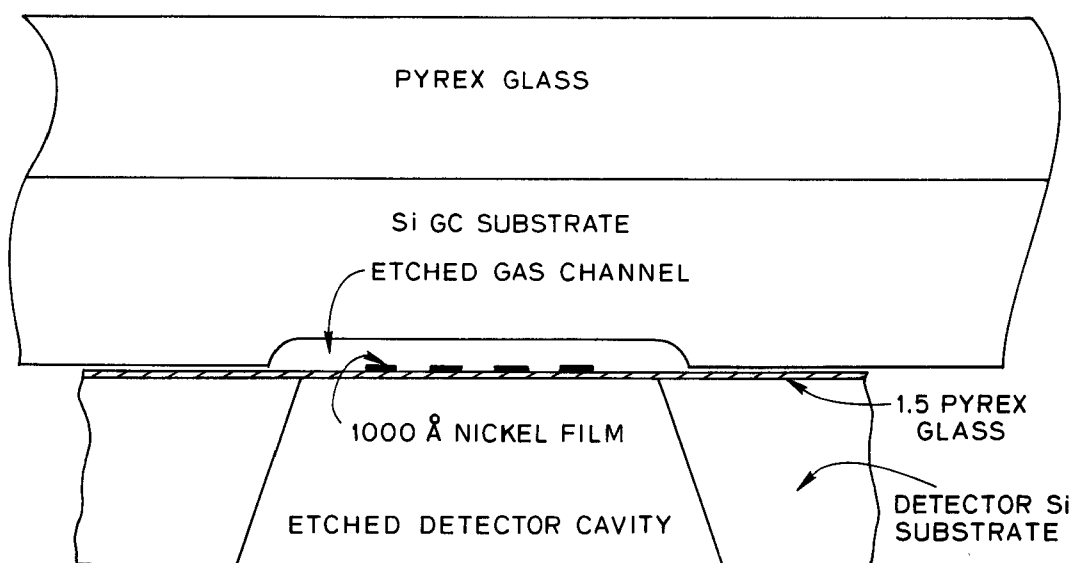
Figure 4.11. DETECTOR CROSS SECTION.

44

and detectivity. The most important parameter for the miniature system
in environmental monitoring applications is detectivity. Assuming that
the detector noise remains constant, the electronic system with the
highest sensitivity will be optimum for the miniature system. Figure
4.12 shows a graph of calculated detector sensitivities as a function of
temperature for the bridge, constant current, and constant temperature
configurations. The choice is basically between constant current and
temperature. The maximum temperature limit for these detectors is about
300°C above ambient, but they are usually operated below this point. The
constant current mode results in the highest sensitivities at higher tem-
peratures due to a thermal feedback effect because of the positive TCR of
the nickel resistors. At a given operating point a sample peak causes
the thermal conductivity of the gas to decrease. This causes an increase
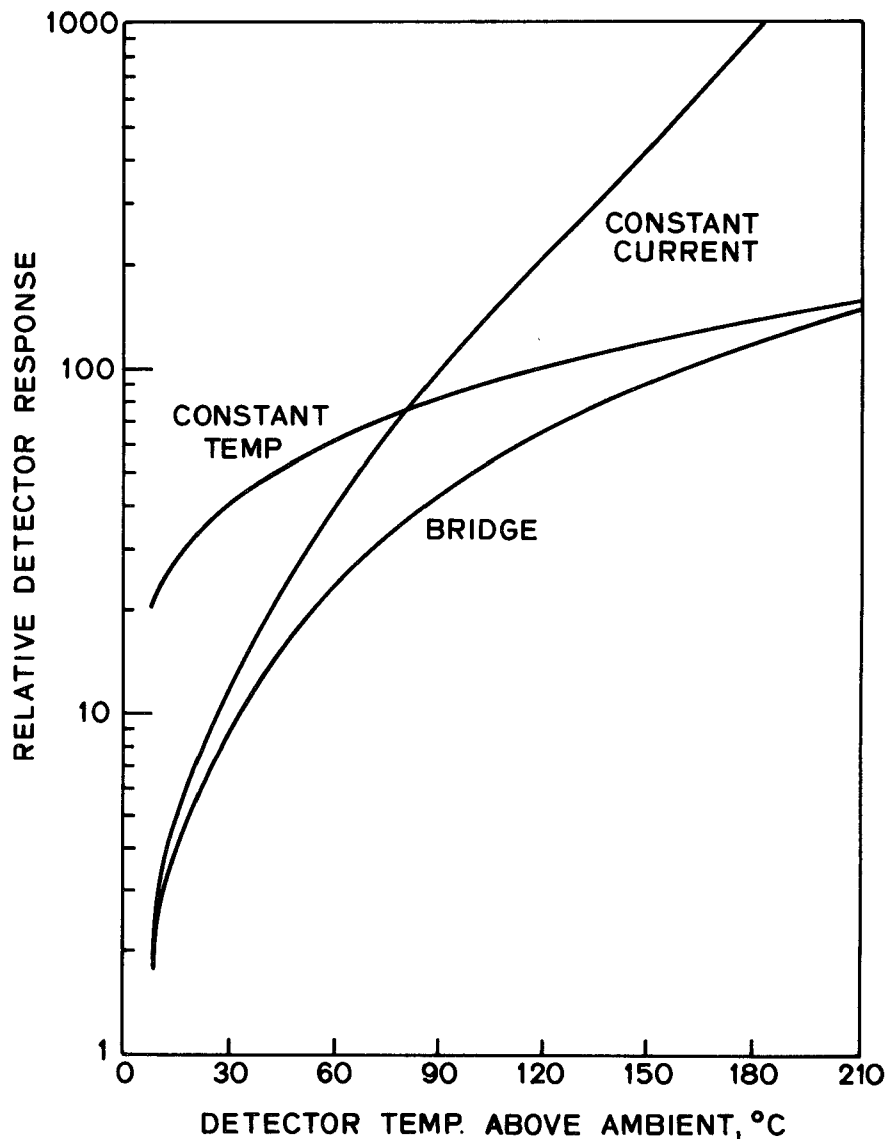
Figure 4.12. RELATIVE DETECTOR RESPONSE FOR THE THREE DETECTOR DRIVING
              SYSTEMS.

45

in the detector temperature which causes an increase in resistance and subsequently an increase in power, $I^2R(T)$, dissipated in the device. This increase in power also increases the detector temperature which again increases sensitivity. This feedback effect is normally stable, unless the operating point temperature is set too high. If the current source can put out unlimited power, then the detector can enter so-called thermal runaway and destroy itself. Normally the characteristics of the current source are designed to limit the maximum power available to drive the detector so this condition is averted. This thermal feedback can cause nonlinear response for very large peaks as described below.

The constant temperature mode can also be used, where the detector voltage is constantly adjusted to keep the detector at a particular temperature. When a gas peak goes past the detector, the voltage drive is reduced, reducing the power dissipated by the detector. This mode is not as sensitive as constant current at moderate (100-200°C) tempeatures, but does prevent thermal runaway.

Basic thermal and electrical theory can be used to calculate the operating point, temperature, temperature excursions, sensitivity, and linearity of the integrated TCD. It is most convenient to assume that the structure is always in thermal equilibrium. The thermal time constant of the device is about 1 ms, much smaller than any peak width, so that the input power to the device always matches the power dissipated by the detector, which is mostly conducted through the carrier gas. In the constant current case the dissipated power is simply $I^2R(T)$. The power dissipated by the detector is approximately $G_0T(1 + \beta T/2)$ where G_0 is the thermal conductance of the combination of carrier gas and detector support and β is the temperature coefficient of thermal conduction of helim. To solve for the detector temperature a form of $R(T)$ must be found. For the nickel films used in these detectors the resistance is quite closely given by

$$R(T) = R_o \exp(\alpha T) \qquad (8)$$

where R_0 is the detector resistance at ambient temperature, and T is the temperature above ambient. For nickel films the TCR, $\alpha = 0.00426$ °C^{-1}, is appropriate to use. To solve for the operating point temperature the equation

$$G_o T \left(1 + \frac{BT}{2}\right) = I^2 R_o \exp(\alpha T) \qquad (9)$$

must be solved. This is usually done numerically, but a graphical solution may be employed for purposes of discussion. The graph shown in Figure 4.13 shows the power dissipated by four constant currents through the detector for a range of detector temperatures to 280°C above ambient. Also plotted is the power dissipated by the detector for those same temperatures. The points of intersection, A, B, and C, are the operating point temperatures for 6, 8, and 10 mA. For the conditions used in this graph,
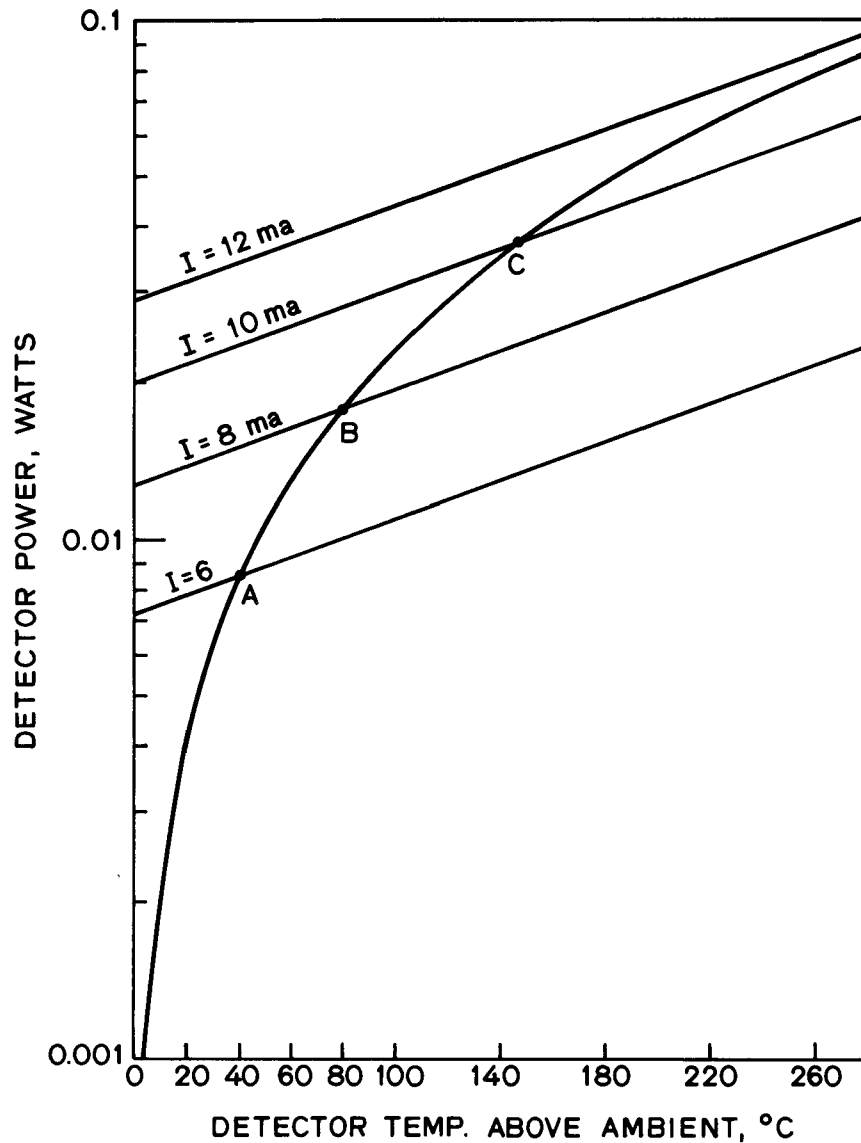
Figure 4.13. GRAPHICAL SOLUTION TO DETECTOR OPERATING POINTS FOR DIF-
FERENT DETECTOR CURRENTS. R_o = 200 Ω, G_o = 0.002 °C/Watt.

R_o = 200 Ω and G_o = 2 x 10^{-3} W/°C, the detector goes into thermal runaway
before 12 mA is reached. This first order theory is sufficient for analyses
of operation below about 200°C above ambient. In fact, the device does
not run away at 12 mA in the above sample because the TCR of the nickel
resistor decreases enough at high temperature to remain in a stable state.

Two of the more important characteristics of the detector are sensitivity
and linearity. The small signal sensitivities are determined by differ-
entiating equations such as (9) to get dV/dC, the change in output voltage
for a small change in sample gas concentration. This is usually done as-
suming that dG/dC, the change in thermal conductance for a given change in
concentration, is constant. These assumptions are generally correct for

gas peaks, but for air peaks the voltage from the detector can double, which can introduce considerable nonlinearities. These nonlinearities in response to large peaks can be computer corrected if a form for the response is known.

In order to find the output voltage of the detector for a given peak concentration, Equation (9) is solved twice, once for the operating temperature T_0, and again for the peak temperature T' when the thermal conductance is reduced by a gas peak to G'_0. The output voltage is then

$$V_0 = IR(T') - IR(T_0)$$

The output voltages for a given change in G_0 have been found for a set of detector currents I and the results are shown in Figure 4.14. Here current is varied as a parameter and the operating point temperature and the output peak voltage are both found. The experimental points are determined by measuring the peak voltage for the same set of currents, and measuring the temperature of the detector by measuring its resistance. The agreement between the points is excellent over a wide range of operating conditions. A wide variety of curves like this can be determined for injected peaks of different sizes.

To determine the linearity of the detector, the output voltage must be found as a function of changes in thermal conductivity, for a fixed detector current. In order to convert these results to output voltage as a function of mole fraction of the sample gas in the carrier gas, the thermal conductance of the gas mixtures must be known. Theoretical results are not sufficiently accurate for most gas mixtures, so experimental results of thermal conductivities of gas mixtures as compiled by Tsedenberg [9] were used. The experimental points for argon in helium were curve fitted as shown in Figure 4.15. This result was used to find the thermal conductivity change for a given argon concentration, which was then used to find the output voltage at a given detector current. The output voltage is then divided by the argon concentration to produce the output detector sensitivity. A graph of theoretical detector sensitivity vs argon mole fraction is shown in Figure 4.16 for a detector current of 12 mA and an operating point temperature of $50^\circ C$ above ambient. The linearity is good over the range from a part-per-million, which is near the lower limit of detectivity of the detector, to a few percent argon in helium, which is near the maximum sample concentration at the detector during the passage of the airpeak.

The mounting of the detector in the output gas stream introduces sources of noise to the system such as mass flow artifacts and flow noise. The detector operates by dissipating heat by conduction through the gas stream. Since the gas is moving past the detector, there is an additional component in the detector heat balance equation given approximately by $C_v \dot{V} T_d / 2$, where C_v is the specific heat of the gas, $\dot{V}$ is the column flow rate, and T_d is the detector temperature above room temperature. At a constant carrier gas flow this heat loss is incorporated in Equation (9)

48
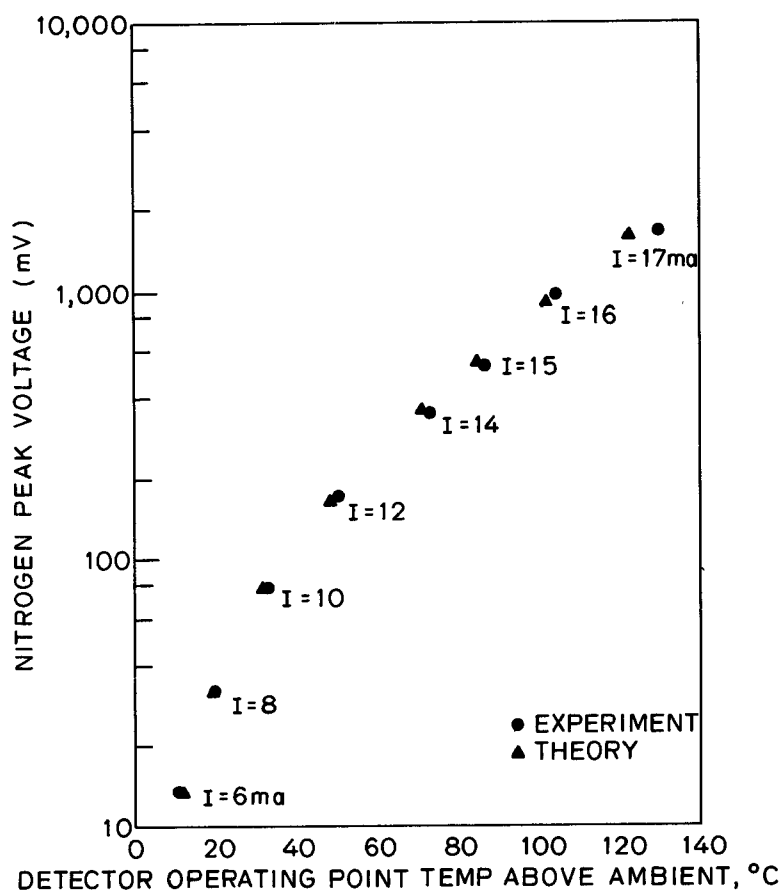
Figure 4.14. DETECTOR OPERATING POINT TEMPERATURE AND NITROGEN PEAK VOLT-
AGE AS A FUNCTION OF DETECTOR CURRENT.

in the G_0 term, but if the magnitude of the gas flow changes, the detector temperature and hence the output signal will change. The flow can change due to either changes in carrier gas supply pressure or at the introduction of higher pressure sample gas at the injection valve. The injection arti-fact can be a rather large signal, at high gain, but is over by the time the air peak reaches the detector. An example of such a signal can just be seen, immediately after injection, in Figure 4.4. The change in signal with carrier gas pressure is noticeable in the prototype instrument, but does not degrade performance. The change in carrier pressure is due to the on/off valve and surge tank arrangement in the miniature carrier gas supply system. The pressure in the surge tank drops about 7 x 10^2 Pa (0.1 psi) during a chromatogram. That drop introduces a drift in the

49
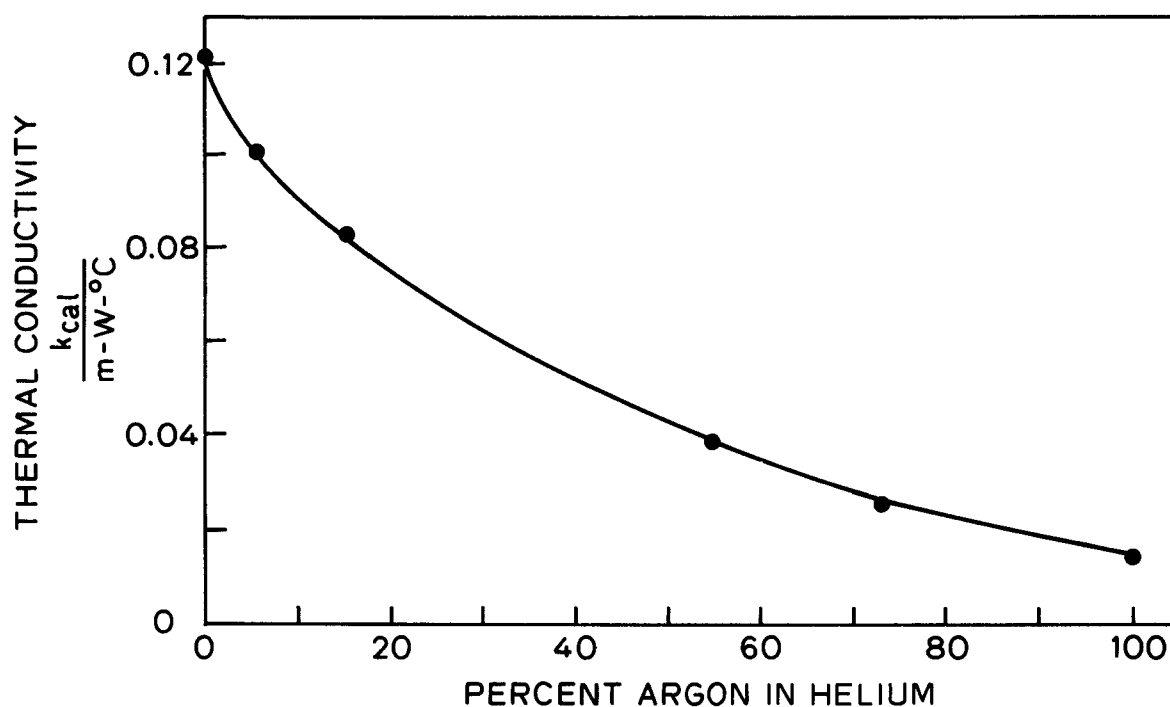
Figure 4.15. THERMAL CONDUCTIVITY OF Ar/He GAS MIXTURES AS A FUNCTION OF THE PERCENTAGE OF Ar IN THE MIXTURE.
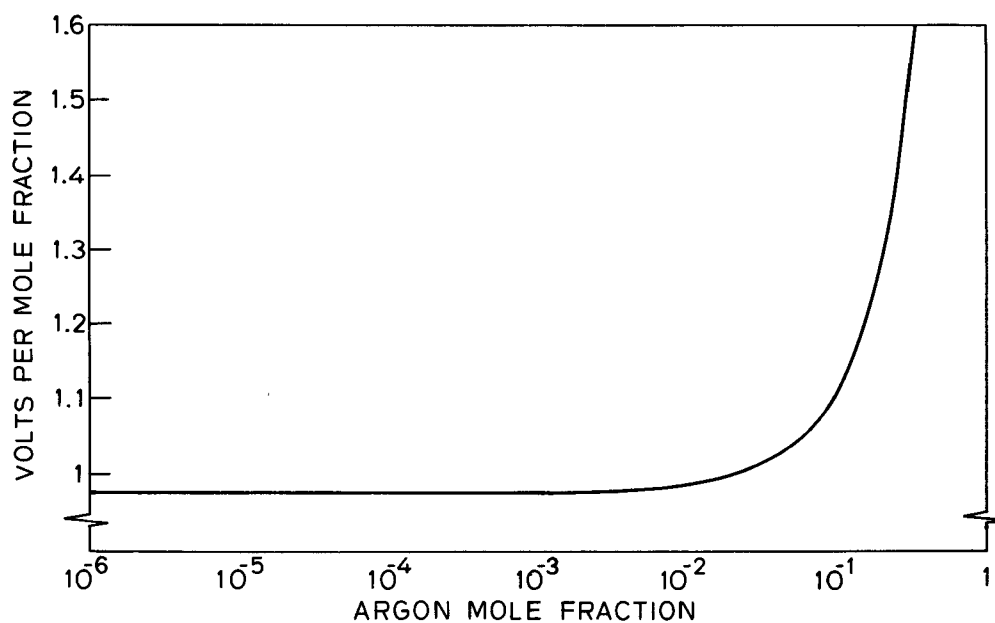
Figure 4.16. LINEARITY OF DETECTOR SENSITIVITY AS A FUNCTION OF ARGON MOLE FRACTION IN THE HELIUM OUTPUT STREAM.

50

detector signal approximately equivalent to the drift introduced by ambient temperature variations. A filtering algorithm in the computer program is used to compensate for these drifts.

The flow of gas past the detector also causes some degree of noise. This noise is thought to be due to extremely slight flow instabilities in the detector gas channel. The flow itself is highly laminar, due to the small dimensions and low gas velocity, but these slight instabilities can be detected as noise. In the prototype instrument electronics, this detector noise is about the $0.5-\mu V$ peak-to-peak level, somewhat under the $2-\mu V$ peak-to-peak noise of the current source and input noise of the detector amplifier. At high detector currents, which produces higher detector sensitivity, the flow noise becomes the dominant noise source of the system.

4.4 COMPUTER SYSTEM

The miniature gas chromatograph described in this report is capable of significant analytical performance. The unique capabilities of the device are realized only when the device is controlled by, and the results analyzed by, a sophisticated computer system. Since the chromatograph can separate and detect up to 10 vapors in less than 10 seconds, the data analysis system must operate quickly and be compact enough for inclusion in a portable package. In addition, in order to make a truly useful instrument, the operation, calibration, data storage and display functions must be convenient and complete. The computer hardware system and its associated program have been designed to fulfill these requirements as completely as possible given the present state of the art in miniature, low power electronics.

The computer system was designed to be as flexible as possible, giving the computer access via the A/D converter to the pressure and temperature sensors and the amplifier outputs which describe the state of the analytical system. The computer has been programmed to use this information to run the system and has a complex data analysis section to process the detector output signal. In addition, a significant portion of the computer program is dedicated to interfacing the electronics system to the user via a keyboard and display. The algorithms and programs necessary to run the system are described in the remainder of this section.

4.4.1 Data Analysis

The most difficult part of the computer program is associated with analyzing the detector output signal. A typical chromatogram is a rather complex signal, especially for a modest computer system. There is often a pressure artifact after injection, a very large air peak, followed by any number of potentially very small gas peaks. The uncontrolled GC temperature introduces considerable drift to the amplifier output along with both flow noise and noise from the electronics. In order to measure the concentration of an output peak the area of the output peak must be measured and compared to the area of the air peak. The major analytical problem is thus reduced to finding the area of a small output peak in the presence of noise and drift.

51

There are a wide variety of methods to detect the presence of small signals in noise. Given some knowledge of the properties of the signal and the noise, it is usually possible to select a system which enhances the ability to measure the desired attribute of the signal and to minimize the effects of the noise on that measurement. In the case of the gas chromatograph, the signal is the detector voltage, which is proportional to the concentration of gas in the output gas stream, and the noise consists basically of random fluctuations in detector output, electrical noise introduced by the amplifier, and a variety of drift components. Due to the chromatographic process, the gas concentration and hence the detector signal, $x(t)$, is quite nearly gaussian shaped with respect to time

$$x(t) = \frac{A_x}{\sqrt{2\pi}\,\sigma_x} \exp\left(-\frac{(t - t_o)^2}{2\sigma_x^2}\right) \tag{10}$$

This gaussian peak can be described as having three distinguishing characteristics, a retention time, t_o, a peak area, A_x, and a standard deviation, σ_x, and all three must be measured by the computer system.

Filtering Algorithm--
In order to perform these measurements, the analytical problem is broken into two parts, a filtering procedure to maximize the signal to noise (S/N) ratio, and an analysis of that filtered data. The filtering procedure was chosen to maximize the ability to determine the existence of, and measure the retention time of, the gaussian peak. Filtering theory is then used to find the optimum way of finding the retention times, t_o. The transfer function $H(\upsilon)$, of an optimum filter is found to be [10]

$$H(\upsilon) = \frac{KX^*(\upsilon)}{Y_N(\upsilon)} \exp(-j2\pi\upsilon t_o) \tag{11}$$

where

$X^*(\upsilon)$ is the complex conjugate of the input Fourier transform

$Y_N(\upsilon)$ is the power spectral density of the noise

K is a constant

In order to solve for the transfer function of an optimum filter, some form of the power spectral density of the noise must be assumed. For this prototype the noise was assumed to be white, that is $Y_N(\upsilon)$ is a constant. For white noise the optimum filter will have the same shape as the input signal, so that in the case of a gaussian input signal the output of the filter would also be a guassian. The standard deviation of the output signal (σ_{out}) would be given by

$$\sigma_{out} = \sqrt{\sigma_{in}^2 + \sigma_F^2}$$

52

where σ_{in} is the standard deviation of the input gaussian signal and σ_F is the standard deviation of the filter in the time domain.

In order to simplify the determination of the location of the signal maxima and points of inflection, a differentiator was included in the filtering algorithm. Differentiation at this stage is tolerable since much of the noise has been removed by the optimum filter.

The overall impulse response of the optimum filter and the differentiator is given by

$$h(t) = \frac{-A_H}{\sqrt{2} \, \sigma_x^3} \, t \, \exp\left(-\frac{t^2}{2\sigma_x^2}\right) \tag{12}$$

This filtering function is graphed as a function of time in Figure 4.17. When the original gaussian peak is operated on by this filtering function, a different output is obtained which is given by the convolutional integral

$$Y(t) = \int_{-\infty}^{t} x(\tau) \, h \, (t - \tau) \, d\tau \tag{13}$$

Using Equations (10), (12), and (13) the filter output signal $Y(t)$, is given by
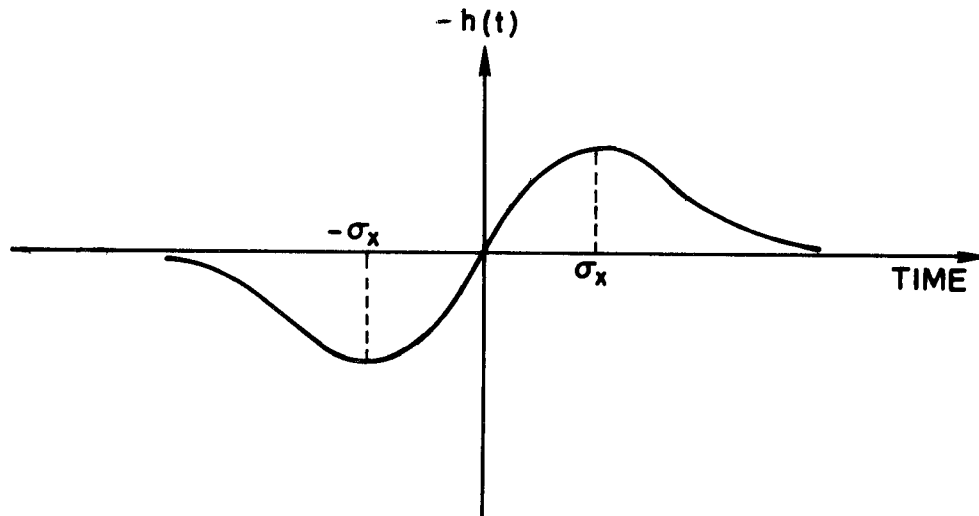
Figure 4.17.   IMPULSE RESPONSE, h(t), OF THE OPTIMUM FILTER.

53

$$Y(t) = \frac{A_X A_H}{\sqrt{2\pi}\ \sigma_y^3}\ (t_o - t)\ \exp\left[-\frac{(t - t_o)^2}{2\ \sigma_y^2}\right]$$

where

$$\sigma_y = \sqrt{2\sigma_x}$$

A_X is the area of the input gaussian

A_H is a constant from Equation (12)

σ_x is the input gaussian standard deviation

This function is shown in Figure 4.18. This is the filtered gaussian wave-form which must be measured to determine the concentration of the gas peak. In order to do that, the original standard deviation, σ_x, and the original amplitude must be reconstructed from measuring this waveform. The standard deviation can be determined from t_{max} and t_{min}, since it can be shown from Equation (12) that $t_{min} - t_{max} = 2\sigma_y$.

Furthermore, the area under the positive portion of $Y(t)$ is

$$S = \int_{-\infty}^{t_o} Y(t)\ dt = \frac{A_X A_H}{\sqrt{2\pi}\ \sigma_y} \tag{15}$$
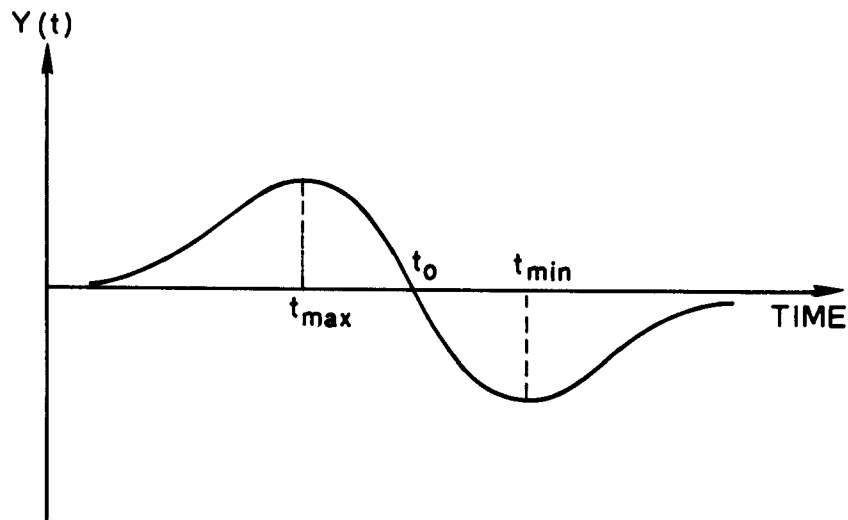
Figure 4.18. THE RESULTANT WAVEFORM AFTER FILTERING A GAUSSIAN INPUT SIGNAL.

so that the original peak area, A_X, can be recovered by performing the calculation.

$$A_X = KS \, \sigma_y \qquad (16)$$

where K is a constant which is the same for all input gaussians. Thus by measuring the area S and t_{max} and t_{min}, the gaussian area can be found. This method is theoretically more reproducible than measuring the area of the original gaussian peak, since much of the noise which could interfere with the integration has been removed by the filtering process.

Filter Realization--
In a digital system, the filtered output signal, Y(t), cannot be determined continuously, but must be calculated at discrete time intervals. This is achieved by first sampling the input waveform by an A/D converter to obtain a number proportional to the input voltage. As the input is repeatedly sampled, a set of numbers is obtained as a function of time. This set is multiplied by a set of filter coefficients which are found by sampling the impulse response of the filter, h(t) at the same rate. Each filtered point is the sum of a large number of sampled points multiplied by the filter coefficients. The larger the number of multiplications performed, the closer the resulting sum will be to the actual value of Y(t).

In a microcomputer realization of the digital filter, the speed at which the multiplications can be performed is the limiting factor. A compromise must be found in the chosen sampling rate of the analog signal, the precision of the numerical representation of the signal, the precision of the filter coefficients, the number of multiplications performed for each sample point, and the way the data points are stored in the computer's memory.

In order to perform the filtering function, the convolutional integral, Equation (13), must be approximated in discrete form as

$$Y_K = \sum_{i=0}^{m} x_i h_{k-i} \qquad (17)$$

where

Y_K are the filtered sample points

X_i are the sampled input data points

h_K are the filter coefficients

The computer program to perform this filtering function is described below.

The digital representation of the detector amplifier signal is stored in the computer memory along with the last 63 such sample points. After each sample is taken and stored, the accumulator is zeroed, every other point

55

is retreived from memory, multiplied by the correct filter coefficient for that point, and the result is added to the accumulator. After 31 such multiplications the number in the accumulator is the filtered result for that set of 64 data points and this result is stored. About 3 milliseconds later another sample command is given, the 64th data point is erased from memory, all previous data points are shifted down one place, and the new data point is stored to begin the process again. This process is shown in graphical form in Figure 4.19. Here the filter coefficients are shown; these are the multipliers of the delayed sample points mentioned above. When the gaussian peak is processed by the filter, the result is shown below. The filter is seen to produce the signal, Y(t), which is nearly the derivative of the input gaussian. The retention time of the peak is the zero crossing point of the output signal, and twice the standard deviation, σ_y, is the positive peak to negative peak time. In order to obtain A_X, the area of the original gaussian, the area S must be found. This is done by a simple point by point numerical integration of the filtered signal.
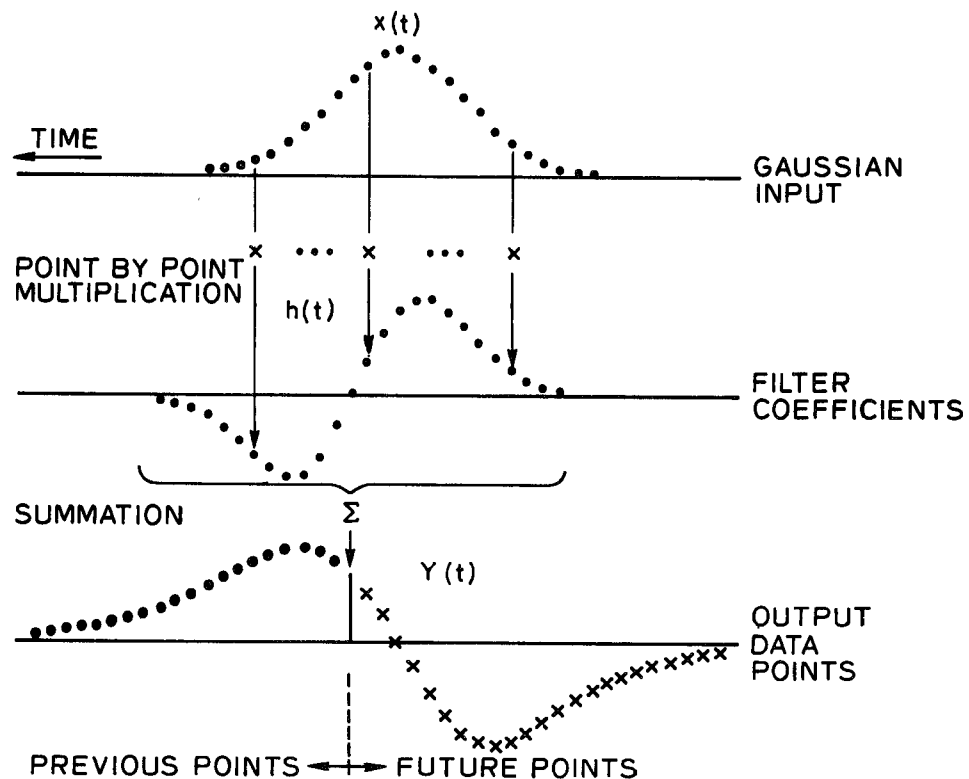
Figure 4.19. GRAPHICAL REPRESENTATION OF THE FILTERING PROCESS. Each output point represents the sum of the point by point multiplication of x(t) and h(t).

This particular filter is optimized for maximum signal to noise ratio at the zero crossing of the signal, so that this point is used by the computer can look at the data and determine the area of the peak at that retention time.

Errors--
In the miniature system the main sources of error in the peak area calculations are due to the finite sampling rate, which limits the precision in finding σ_y, if σ_y is calculated directly from t_{min} and t_{max}. Since there are usually only about 30 sample points between t_{min} and t_{max}, an uncertainty of one sample point is about a 3% error. In the presence of noise, the uncertainty is increased due to nonideal waveforms. There are basically three ways to improve this performance. Conceptually the eariest is to sample more frequently, which would increase the number of points between t_{min} and t_{max}, and thus improve the resolution of determining σ_y. In order to achieve large increases in performance, however, the computational speed would have to be proportionally increased. The microprocessors necessary to perform these calculations are not presently available, so this solution is not now feasible. The other two methods use interpolating filters or curve fitting to achieve effectively greater time resolution than the sampling interval. The curve fitting procedure was found to be very helpful, but is very time consuming, taking many seconds per peak area calculation. This is not desirable for the portable instrument. It is also possible to use a class of interpolating filters to increase the effective time resolution. This procedure seems to be the most promising to increase the accuracy of the σ_y determination and thus the area measurement, and it will be investigated at the earliest opportunity.

An additional source of error is due to the action of the differentiator in the filtering algorithm on the input signal. In the presence of drift, the differentiator will change the drift into an offset. This offset shifts the position of the zero crossing of the filter output signal. For peaks with large retention times and low amplitude, the baseline offset signal may be so large that no zero crossing is detected. The computer program will be modified in the future to compensate for this baseline offset to increase ability to detect the later peaks.

Filter Simulation--
The effectiveness of the filtering system can be seen in the computer simulation results shown in Figure 4.20. The top output shows a gaussian peak plus 1/f noise before the filtering,and the lower output is after the filtering algorithm. A computer simulation is useful in analyzing the performance of the filter since the amplitudes of the peak and the noise can be easily adjusted and the "retention time" of the gaussian peak is exactly known. The filter parameters and standard deviations can also be changed to characterize the filter over a wide range of conditions. A systematic characterization of various filtering and area algorithms will be the subject of a forthcoming report.

Peak Finding--
The filtering scheme mentioned is designed to increase the signal to noise ratio of the detector output signal and thus make it easier for the computer to locate and measure the peaks. The filtering process is a part of a section of the program dealing with finding and measuring the peaks. A simplified flow chart of this program is shown in Figure 4.21. The main criteria for locating a peak is the steep zero crossing in the filtered data. If a positive maximum above a threshold is found in a time window, followed by a zero crossing, a peak is said to occur. It is not until the zero crossing, however, that the computer has determined that a peak exists,
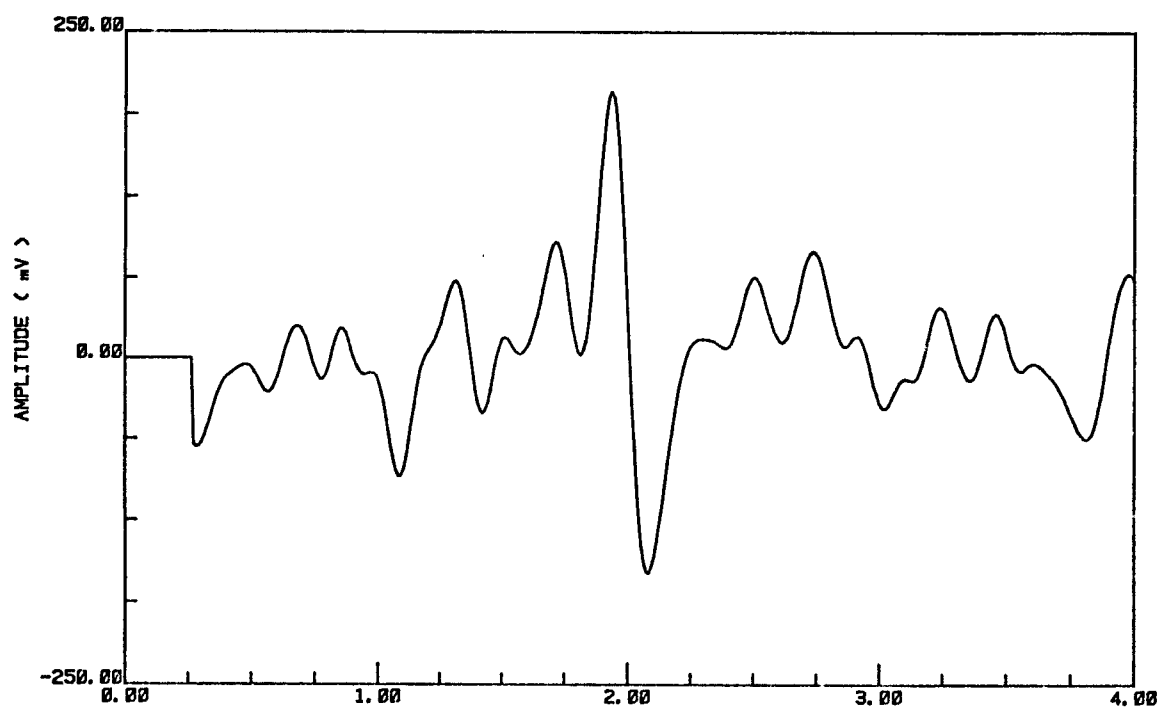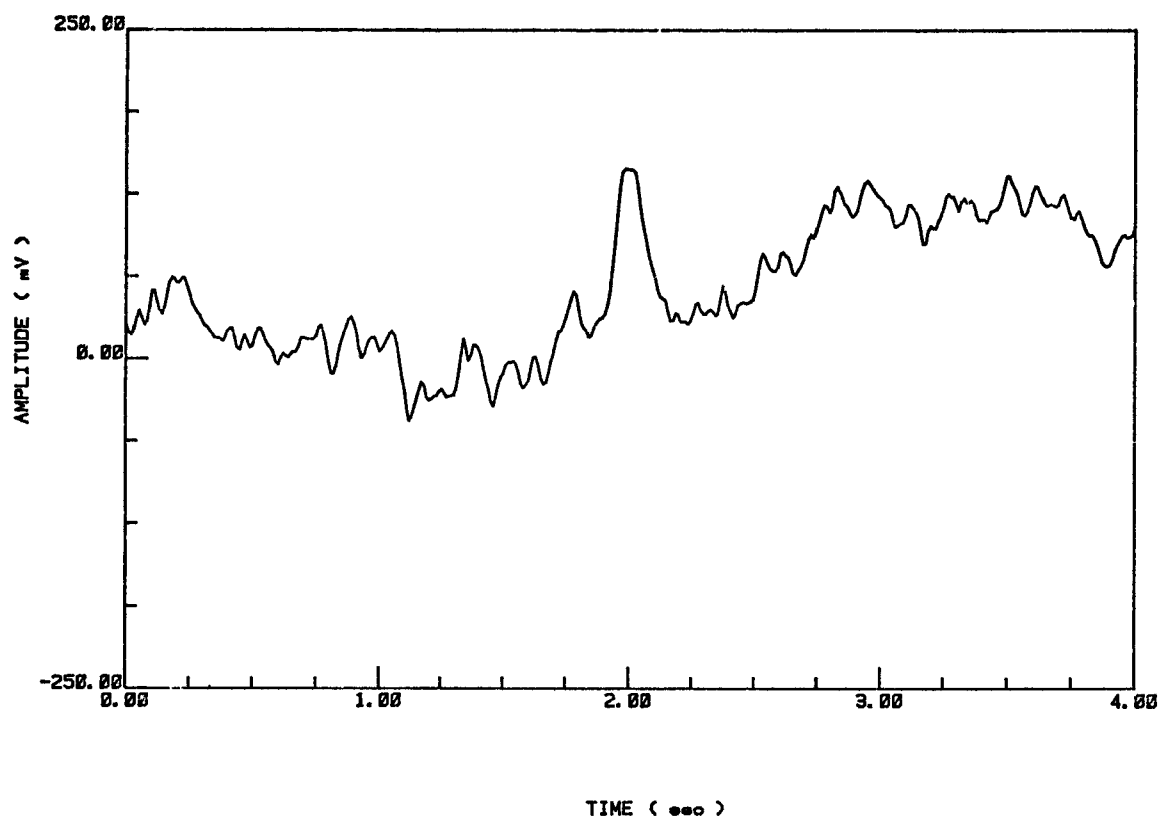
Figure 4.20.   COMPUTER SIMULATION OF GAUSSIAN PEAK WITH NOISE.   (a)   Before
filtering; and (b) after filtering.

58

PEAK ANAYLSIS FLOW

```
              ┌──────────────┐
         ┌───▶│  SAMPLE DATA │
         │    │  AND FILTER  │
         │    └──────┬───────┘
         │           ▼
         │         ╱ TIME ╲
   NO    │◀───────◀ WINDOW ╲
         │         ╲      ╱
         │           │ YES
         │           ▼
         │         ╱VALID╲      YES
   NO    │◀───────◀ PEAK  ╲──────────┐
         │         ╲  ?  ╱           │
         │           │               │
  ┌──────┴──────┐  ┌────────────────┴────┐
  │ GET RET. TIME│  │ INTEGRATE PTS &    │
  │ OF NEXT PEAK │  │ DETERMINE SIGMA    │
  └──────┬──────┘  └──────┬─────────────┘
         ▲                │
         │      ╱  END  ╲ │
   NO    └─────◀CHROMATOGRAM
                ╲   ?   ╱
                   │ YES
                   ▼
           ┌──────────────────┐
           │ AREA CALCULATIONS│
           │   AND DISPLAY    │
           └──────────────────┘
```
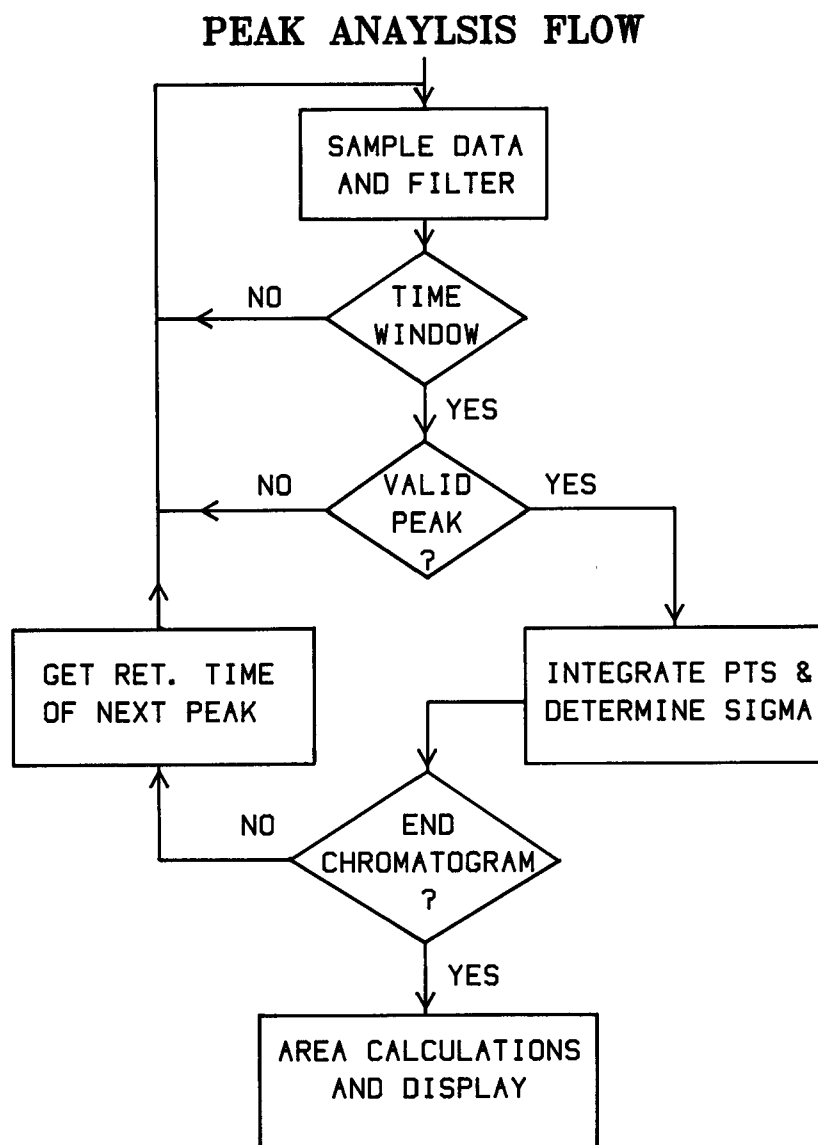
Figure 4.21. FLOW CHART FOR PEAK FINDING AND AREA CALCULATIONS.

and at that point half of the filtered peak data has already been calcu-
lated. The computer thus needs to continuously store the filtered output
points so that the data is available when a legitimate zero crossing is
found. After the zero crossing, the second half of the peak data is also
stored, and the complete peak data is later analyzed by the peak area calcu-
lation program.

Swept Time--
In order to achieve maximum benefit from the filter, the standard deviation
of the filter should be very close to that of the input gaussian peak. In
a chromatogram this is very rarely the case. The air peak is quite narrow,
with a standard deviation of about 20 ms. For a peak with a long retention
time, the standard deviation can increase by a factor of five or more. Such

a wide peak would not be matched to the characteristics of the filter and the benefits of the filtering would be substantially reduced. It is not practical to change the filter characteristics during the course of the chromatogram, so "time" is changed instead. The sampling period is linearly increased during the chromatogram so that each peak is a constant number of sampled points wide. This then guarantees effective filtering for all of the peaks at the slight disadvantage of having to convert from sample point units to real time for all retention time calculations. This process of changing the sampling rate has been called "swept time". The match between standard deviation increase and linearly increasing period is quite close, so that this swept time algorithm is well suited to the needs of the portable chromatograph.

4.4.2 Operating Program Flow

The peak finding section is a part of a larger program which operates the system. As shown in diagram form in Figure 4.22, the program proceeds as follows. Upon a signal to start an analysis the computer first takes a reading of the column temperature. This is used mainly to calculate the expected retention times of the sample peaks of interest for that chromatogram. Time windows are then set up so that the computer knows where to look for the zero crossing of a peak. The high gain amplifier is zeroed to take care of any amplifier zero drift since the last analysis and the high pressure valve in the carrier gas supply is opened to charge up the

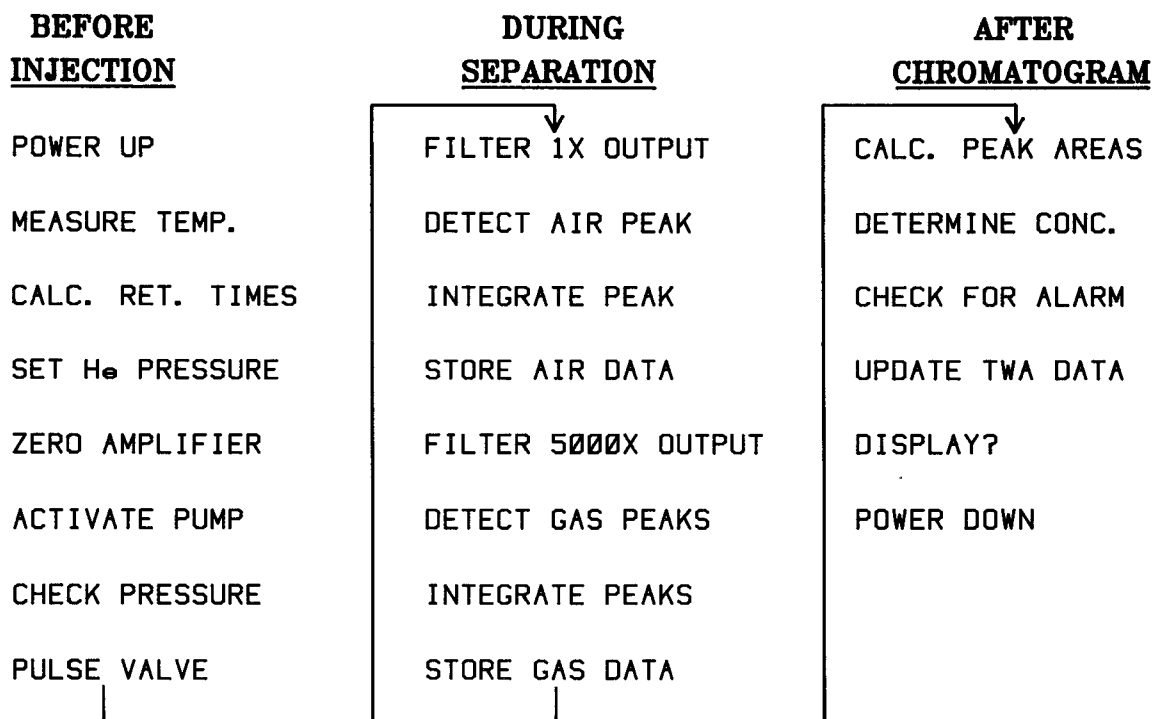| BEFORE INJECTION	DURING SEPARATION	AFTER CHROMATOGRAM
POWER UP	FILTER 1X OUTPUT	CALC. PEAK AREAS
MEASURE TEMP.	DETECT AIR PEAK	DETERMINE CONC.
CALC. RET. TIMES	INTEGRATE PEAK	CHECK FOR ALARM
SET He PRESSURE	STORE AIR DATA	UPDATE TWA DATA
ZERO AMPLIFIER	FILTER 5000X OUTPUT	DISPLAY?
ACTIVATE PUMP	DETECT GAS PEAKS	POWER DOWN
CHECK PRESSURE	INTEGRATE PEAKS	
PULSE VALVE	STORE GAS DATA	

Figure 4.22.   SIMPLIFIED FLOW CHART OF THE MAIN PROGRAM.

60

pressure regulator surge tank to the correct pressure. The computer monitors the pressure sensor on the surge tank until the desired pressure is reached, when it closes the high pressure valve. The computer then signals the sample pump to withdraw, pulling in an atmospheric sample through the sample input system. By monitoring the pressure drawn by the sample pump, the computer determines when the pump has finished drawing in the sample. The pump is then reversed, pressurizing the sample. When the desired sample pressure is reached, the computer fires the injection valve, which introduces the sample to the head of the separating column. The computer then starts sampling the detector output through the A/D converter. Just before the air peak is expected, the swept time circuitry is activated, which begins to lengthen the signal sampling period. After the air peak is detected the computer switches to the high gain amplifier output and starts searching for peaks. When a timer expires signaling the end of the chromatogram, the computer computes the area of the peaks, calculates the respective concentrations, updates the appropriate maximum and TWA concentration registers, and then shuts itself off, awaiting a command from the keyboard or the automatic timer.

Calibration Routine--
It is possible for this machine to perform an automatic calibration cycle. It has been programmed to automatically find and measure the retention time of a gas peak and store the retention time and amplitude calibration factors in memory. To calibrate the machine for a particular gas, that one gas is connected to the input of the instrument and the calibration routine is selected. The temperature coefficient for that gas must be previously entered, along with the known concentration of the calibration gas. The computer then performs the analysis and updates all pertinent calibration coefficients.

This simple routine should reduce the amount of periodic service of the device for calibration purposes and allows for on-site calibration to insure the accuracy of the portable instrument.

Keyboard and Display Program--
For the prototypes, a simple keyboard and display were desired. The amount of front panel space is limited so a large keyboard is not practical. A 16-switch keyboard was chosen along with a 4-digit display. When coupled to the computer these limited devices are capable of a number of functions.

In the prototype instrument a large number of the internal parameters are capable of being changed or updated by the user. There are 10 system parameters plus 9 gas parameters for each of 10 different gases which can be displayed or changed by the user. In addition there is a calibration mode, normal sampling mode, and automatic sampling mode which can be selected. A simplified chart of the keyboard routine is shown in Figure 4.23. When the machine is in its quiescent state, it is waiting for a function key, either A, B, C, D, or E. If A is pushed the machine begins a new analysis. B is used for displaying and changing the system parameters. For example, if B and then 1 are pushed, system parameter 1, the gas peak threshold, is displayed. C is used to change the value of a gas parameter. A sequence here might be to change the temperature coefficient of gas number 5. The button sequence would be C, 5, and then 3, the button 3 for the temperature parameter. The display would then zero, waiting for the new value to be entered. To input .00029, for example, the button

COMMAND	FUNCTION	DESCRIPTION
A	Survey mode	The machine performs one sample analysis and updates concentrations of programmed gases.
B	System parameter display/change	To display a system parameter the parameter is entered. After the parameter is displayed, pressing 3 will allow the user to change that parameter.
C	Gas parameter change	To change a gas parameter, the gas # and parameter # are entered, followed by the new value for that parameter.
D	Gas parameter display	Entering the gas # followed by parameter # displays the value of that gas parameter.
E	Sample calibration	In this mode the machine determines the overall concentration multiplier and retention time "A parameter" of the gas under calibration. After choosing a # for the gas, the known concentration of the calibration gas is entered. The machine then performs one analysis and updates the necessary parameters.

Automatic Mode: The machine samples the atmosphere and updates maximum concentration and TWAs of programmed gases with the sampling interval specified by system parameter 7.

Figure 4.23. KEYBOARD COMMAND DESCRIPTION.

sequence F,0,0,0,2,9,F is used, the first F is interpreted as a decimal point and the last F is an enter button to tell the machine that the number is complete. The D button is similar to the B, but for display of the gas parameters. The sequence D15, for example, displays the concentration of gas 1. The last button, E, activates the calibration routine; the sequence E 4 1000 calibrates gas 4 at 1000 ppm. A complete list of the function keys and gas and system parameters is listed in Figure 4.24. Mistakes are cleared by simply pressing another function key instead of the "enter" button. The 4-digit display can show up to a 10-digit number by shift keys which move the display one place to the right or left. Since many of the displayed numbers are betwen 9999 and 0.001, this shift is not always required.

Power Down--
The present digital electronics system uses a Z-80A microprocessor, six EPROM's, four RAM's, plus a number of support chips. During operation the device consumes about 300 mA at 5V, or 1.5 W. In order to save power a novel power down system for the digital electronics is used. The general scheme is to power the microprocessor only during those times that is actually computing, and to power down whenever it is waiting for a keyboard entry. This system also works in between key strokes from the

GAS PARAMETERS

Parameter Number	Definition
0	Select/deselect flag
1	Retention time "A parameter"
2	Retention time "B parameter"
3	Overall concentration calibration multiplier
4	Overall concentration correction with temperature
5	Concentration
6	Time weighted average concentration
7	Maximum concentration detected
8	Alarm level
9	Reserved

SYSTEM PARAMETERS

Parameter Number	Definition
0	Maximum chromatogram length
1	Gas detection threshold
2	Carrier pressure
3	Valve injection pressure
4	Thermistor constant V_ϕ
5	Thermistor constant β
6	Thermistor constant $1/T\phi$
7	Automatic mode wait timer
8	Swept time $t\phi$
9	Swept time $1/\alpha$

Figure 4.24.   GAS AND SYSTEM PARAMETER LISTING.

keyboard. For example, when the computer finishes a chromatogram, it stores the appropriate concentrations in nonvolatile CMOS memory and then turns off power to itself. When a concentration is requested from the keyboard, the D button is pushed, which produces a signal which turns on power to the microprocessor. The computer recognizes the button, goes to the display part of the program and then turns power off again. The entire button pushing sequence takes about 1 ms, which is the amount of time the microprocessor draws power. As each additional button is pressed, the machine continues to immediately power down. After the desired

concentration is displayed, the computer again powers down; the number is retained in the display driver and continues to be displayed. This power down system has allowed the battery size to be significantly reduced without sacrificing instrument performance.

Future Improvements--

The computer system incorporated in this portable instrument represents the most advanced possible system given the present state of electronic development. A number of improvements are foreseen using components which are either announced for future delivery, or can be reasonably expected to be available in the next year or two. One such product is a low power Z-80A. A product essentially equivalent and software compatible with the present Z-80A but requiring only 20% of the power should be available in 1981. Along with lower power memory and support circuits also soon to be available, the battery required to drive the digital system can be further reduced without reducing performance.

New digital signal processing devices are just being introduced. These devices are basically special purpose microprocessors, optimized for the multiplications and divisions of high precision numbers which is most important for signal processing applications. A device such as these could be used to prefilter the signal, freeing the microprocessor from this job. The microprocessor could then use a more elaborate peak detection program, and since it would not have to perform the filtering, the sampling rate of the detector signal could be increased which would increase accuracy.

There are some changes and additions to the signal processing algorithms which should be included in future versions of the instrument. The baseline drift problem needs additional study to more reliably locate peaks with long retention times. In this prototype the problem of overlapped peaks has not been addressed. The filter used to reduce noise has been designed to be optimum in the presence of white noise. It appears that the actual power spectral density of the noise decreases with frequency proportionally to the reciprocal of the frequency, "1/f noise". This will require some changes in the filtering function to obtain an optimum filter.

There are also improvements likely in the keyboard, display, and interface circuitry which will increase the operator convenience and allow the instrument to automatically output the concentration data taken during a day to a larger computer for further processing, storage, or hard copy display. A larger computer could also periodically monitor the performance of the instrument, pointing out long-term changes in the calibration, or troubleshooting the device in cases where repairs are needed.

5. CONCLUSION

A prototype miniature gas analysis system has been designed and built using a combination of new technologies. The techniques of integrated circuit processing have been utilized to miniaturize the components of a gas chromatography system to a size which is compatible with a portable package. The electronics system used in the gas analyzer is made from recently introduced, state-of-the-art microprocessor, memory, interface, and analog circuits. The combination of devices results in a portable instrument with unique capabilities.

Some of the significant capabilities of the prototype instrument are:

(1) Automatic atmospheric analysis for 8 hours.

(2) Measurement of the concentration of 10 different toxic gases simultaneously.

(3) Concentration information within 30 seconds of sampling.

(4) Concentration measurements from the sub-10 ppm to the more than 1000 ppm level.

(5) Reproducibility within +5% at the 95% confidence level for several substances between 100 and 1000 ppm.

(6) Calculate and store the time-weighted-average and peak concentration for each of the gases.

(7) Convenient display of any concentration or system calibration factor.

(8) Sound an alarm when any gas concentration exceeds a preset maximum value.

(9) Provide automatic calibration for any gas within the instruments measurement range.

(10) Relatively small size and weight for convenient portable operation.

The miniature gas chromatograph performs the actual separation and detection of the constituents of the gaseous sample. It consists of a 1.5-m long separating column, a sample injection valve, and a thermal conductivity detector all of which are integrated on a 5-cm diameter silicon

wafer. The column is formed by etching a long spiral groove on one surface of the silicon wafer and the groove is converted to a tube by hermetically sealing a Pyrex glass cover plate to the silicon surface. The integrated sample injection valve consists of a solenoid actuated diaphragm valve in conjunction with an etched silicon valve seat and orifice.

The integrated thermal conductivity detector consists of a miniature nickel film resistor supported in the output gas stream by a glass and silicon structure. All of the components of the chromatograph are fabricated using novel "micromachining" techniques.

A small servo-driven syringe pump serves to draw in the air samples from the environment and pressurize them for injection into the column. The helium carrier gas for the chromatograph is supplied in replaceable 15-cm^3, high pressure gas cartridges. The gas is delivered by a miniature pressure regulator consisting of an integrated silicon valve, resistive gas path, pressure sensor, and 15-cm^3 surge tank. Both the sample pump and regulator are under the direct control of the computer.

An advanced computer system controls all aspects of the operation of the instrument. The system consists of a powerful microprocessor chip, program memory, data memory, an analog-to-digital converter, a keyboard, and display. The computer controls the automatic sequence of events which cause the instrument to periodically inject atmospheric samples to the GC. As the separated sample peaks evolve from the chromatograph, the computer filters the data to remove noise, measures their retention times for purposes of identification, and determines the concentrations of the gases in the atmospheric sample. This data is used to update the peak and TWA concentrations of the 10 selected contaminant gases.

The instrument is capable of operation in two different modes. The device can be used as a survey instrument, for rapid and accurate sampling under command of an industrial hygienist. In this mode the instrument is instructed to take an atmospheric sample. After about 30 seconds the analysis is complete, and concentration information is immediately available for any of the 10 selected contaminants. This rapid analysis should prove useful in determining the location and extent of potentially harmful conditions around a work place. The instrument is also designed to perform automatic analyses at about 1.5 minute intervals. The device can then be used to record the TWA exposure and peak concentrations encountered by a mobile worker during an 8-hour shift. In this mode an alarm is activated whenever the concentration of a gas exceeds a preset value, warning the worker immediately of potentially dangerous situations.

Realization of the miniature GC gas analysis system is another example of the benefits made possible by the constructive application of silicon integrated circuit processing techniques to problems in diverse fields. The instrument should greatly expand the ability to monitor workers' exposures to toxic gases and therefore aid in the reduction of such exposures, and provide better epidemological data in future health studies. In such an application, the device should prove to be a useful analytical tool and should have significant impact on the fields of industrial hygiene and occupational safety.

REFERENCES

1. Terry, S.C., J.H. Jerman, "A Feasibility Study of a Pocket-Sized Gas Chromatographic Air Analyzer," Stanford Electronics Laboratories, TR No. 77-027, Stanford University, Stanford, Calif., 1977.

2. Terry, S.C., "A Gas Chromatography System Fabricated on a Silicon Wafer Using Integrated Circuit Technology," Ph.D. dissertation, Stanford Electronics Laboratories, TR No. 4603-1, Stanford University, Stanford, Calif., 1975.

3. Concus, P., "On the Liquid Film Remaining in a Draining Circular Cylindrical Vessel," J. Physical Chemistry, Vol. 74, 1970, p. 1818.

4. Bouche, J., M.J. Verzele, Gas Chromatography, Vol. 6, 1968, p. 501.

5. Golay, M.J.E., "Theory of Chromatography in Open and Coated Tubular Columns with Round and Rectangular Cross Sections," in Gas Chromatography (Desty, ed.), Butterworths, London, 1958, p. 36.

6. Dick, R., C.H. Hartman, "Critical Evaluation of the Response Characteristics of the Hydrogen Flame Detector," Varian Aerography Technical Bulletin, pp. 133-167.

7. Driscoll, J.N., et al., "Applications of a Gas Chromatograph Employing an Integrated Photoionization Detector," American Laboratory, Jan 1980, pp. 84-93.

8. Kern, H., M. Elser, "Trace Gas Analysis by a New High Sensitivity Thermal Conductivity Detector," Mikrochimica ACTA, Vol. I, 3-4, 1978, pp. 319-328.

9. Tsederberg, N.V., Thermal Conductivity of Gases and Liquids, MIT Press, Cambridge, Mass., 1965.

10. Papoulis, A., Signal Analysis, McGraw-Hill, New York, 1977, pp. 324-327.

GLOSSARY

A/D converter - analog to digital converter - a device capable of con-
        verting an analog signal into an equivalent numerical value

algorithm - a numerical procedure used for solving a mathematical problem

anisotropic - an etch which has a directional dependence, usually caused
        by the crystalline nature of the substrate

CMOS - complementary metal oxide semiconductor - a semiconductor process
        used to produce devices with very low power dissipation

column - the long narrow tube in gas chromatography used to separate a
        gaseous sample

digital filtering - a procedure used to remove unwanted signals from a
        signal by numerical manipulation of the data

EPROM - electrically programmable read only memory - a program storage
        device

effective plates (N) - a measure of efficiency of a GC column

GC - gas chromatography - a process used to separate and measure the
        constituents of a gaseous sample

microcomputer - a small scale electronic programmable system for the
        manipulation of data

microprocessor - a single computational device which is the main arith-
        metic and logical element in a microcomputer system

nl - nanoliter - 1×10^{-9} liter - a volume equal to a cube 100 μm on a
        side

OV-101 - a trademark for a silicone oil GC capillary column lining
        material

partition coefficient, K - the ratio of solute vapor to stationary phase
        concentration

partition ratio, k - the ratio of adjusted peak retention time to air
        peak time

plate height (HETP) - a measure of efficiency of a column; see Section 4.2.3

program - the set of stored instructions for a computer system

RAM - random access memory - the temporary data storage elements in a computer system

SEM - scanning electron microscope

TWA - time weighted average

DEPARTMENT OF HEALTH AND HUMAN SERVICES
PUBLIC HEALTH SERVICE
CENTERS FOR DISEASE CONTROL
NATIONAL INSTITUTE FOR OCCUPATIONAL SAFETY AND HEALTH
ROBERT A. TAFT LABORATORIES
4676 COLUMBIA PARKWAY, CINCINNATI, OHIO 45226

Third Class Mail

U.S.MAIL

DHHS (NIOSH) Publication No. 81-115